THE DESIGN AND IMPLEMENTATION OF AN EFFECTIVE VISION-BASED LEADER-FOLLOWER TRACKING ALGORITHM USING PI CAMERA

Songwei Li

Thesis Prepared for the Degree of

MASTER OF SCIENCE

UNIVERSITY OF NORTH TEXAS

August 2016

APPROVED:

Yan Wan, Major Professor
Xinrong Li, Committee Member
Shengli Fu, Committee Member and Chair of the Department of Electrical Engineering
Costas Tsatsoulis, Dean of the College of Engineering
Victor Prybutok, Vice Provost of the Toulouse Graduate School

Li, Songwei. *The Design and Implementation of an Effective Vision-Based Leader-Follower Tracking Algorithm Using Pi Camera*. Master of Science (Electrical Engineering), August 2016, 44 pp., 28 figures, 14 numbered references.

The thesis implements a vision-based leader-follower tracking algorithm on a ground robot system. One camera is the only sensor installed the leader-follower system and is mounted on the follower. One sphere is the only feature installed on the leader. The camera identifies the sphere in the openCV Library and calculates the relative position between the follower and leader using the area and position of the sphere in the camera frame. A P controller for the follower and a P controller for the camera heading are built. The vision-based leader-follower tracking algorithm is verified according to the simulation and implementation.

ACKNOWLEDGEMENTS

First, I would like to offer my sincerest gratitude to my major advisor Prof. Yan Wan, who has supported me throughout my M.S. study with her great patience, encouragement and mentoring. My sincere thanks also go to the rest of my thesis committee: Prof. Shengli Fu and Prof. Xinrong Li for their insightful comments and encouragement. I would also like to thank all of my friends for their company, support, and discussion.

I would also like to thank the Toulouse Graduate School at UNT, and Dr. Wan's grants from the National Science Foundation under numbers of GF 1453722, GF 1522458 and GF 154483 for the financial supports.

TABLE OF CONTENTS

Page

CHAPTER 1

INTRODUCTION

1.1 Motivation

UAVs are envisioned to play a big role in disaster rescue, with their capabilities such as information transmission at a long distance, searching in a disaster area, and surveillance of the target in the air or on the ground. In the article [1], a drone-to-drone communication system was built to transfer information at a long distance for a catastrophe scenario. Through the drone-to-drone communication system, real-time video of the disaster zone can be transmitted to the rescue center. Drones sometimes need to work with robots on the ground to scan the disaster area so to get close to a target to obtain the detailed information, in scenarios such as earthquake or the catastrophe of a chemical factory. In these cases, the drone can bring a robot with a camera to the disaster area. Then the drone drops the robot on the ground and follows it using the camera equipped on the drone. Meanwhile, the drone transfers the real-time video from both cameras to the rescue center.

Motivated by the above scenarios, our goal is to make the follower drone track the leader robot as much as possible, as the air-to-ground communication requires the robot to be within a distance to the drone. In this research, we address the leader-follower tracking problem using camera vision. As the preliminary effort, we implemented the vision-based tracking algorithm on a ground robot system, and leave the implementation on the drone platform to the future work.

1.2 Overview of the Thesis

The remainder of this thesis is organized as follows. Chapter 2 reviews two approaches to leader-follower tracking problem using camera vision and analyzes their defects that motivated this research. One approach is to use the area of the sphere in the camera frame to

track the leader target. The other is to use the positions of three features in the camera frame to locate the leader target and then achieve the leader-follower tracking task. Chapter 2 also justifies a key assumption to this thesis, that one camera installed on the follower can determine the position of a sphere ball installed on the leader.

Chapter 3 describes our method for tracking one sphere ball using camera vision and a proportional controller in the leader-follower tracking system. In this chapter, we first describe the algorithm to locate the sphere ball using camera vision, then provides the model of a differential drive robot, and finally describe the control algorithm to implement the follower to track the sphere target.

Chapter 4 describes the simulation and implementation of our leader-follower tracking algorithm described in Chapter 3. The chapter also provides the information of the hardware and software used in the research.

Finally, Chapter 5 includes a conclusion and a brief discussion of future works.

CHAPTER 2

ANALYSIS OF TWO EXISTING APPROACHES FOR OBJECTS' POSITION USING CAMERA VISION

2.1 Introduction

Our goal is to build a leader-follower tracking system using camera vision. To track the leader, the follower needs to obtain leader information using its own camera, such as estimated velocity and angular velocity of the leader, the relative position of the leader and follower, and the bearing angle between the headings of the follower and the leader. Since the velocity and angular velocity of the leader and the bearing angle can be inferred from the relative position, the relative position is an key quantity to estimate for leader-follower tracking algorithm. Through the geometry relationship between cameras on the follower and features on the leader, the relative position of robots can be calculated, as shown in these papers [2]-[6]. Motivated by implementation concerns of this project, we try to develop a tracking algorithm with minimal hardware and feature usage. In particular, when drones and robots search a disaster zone, they need to load batteries, sensors, microcontrollers, and antennas so that there is little space left for cameras or multiple well-separated features on their frames. Meanwhile, the lighter weight can prolong the running time of drones and robots. As a result, we aim to use the minimal number of cameras and features to complete the tracking task.

In paper [5][4], Davison and Murray calculate the object's position using two cameras and one feature. In paper [6], Fang et al describe an approach to calculate the objects' location using one camera and four features on one plane. In consideration of the load limitation of robots and the implementation inconveniences, the number of cameras and features in paper [5],[6]doesn't match our requirement of using a minimal number of cameras and features in our research.

In paper [7], an object's relative distance, which is scaled by the area of one feature (a ball) in the camera frame, is obtained using one camera and one feature (a ball). When the area of the ball decreases in the camera frame, it means the ball is moving away from the camera, or the ball is approaching the camera. This approach didn't provide the relative position between the camera and the ball. In this thesis, we call the method location-feature-area. In paper [8], Chen and Jia use one camera and three features to estimate the leader's position. The location method uses the positions of three features in one camera view. This approach is referred to as location-feature-position in this thesis. Although the location-feature-area and location-feature-position better match with our requirement compared to [5] and [6], they are still not suitable for our research. As the location-feature-area method cannot provide the relative position between the camera and the ball, we cannot build an advanced controller to improve the performance of the leader-follower tracking system for our research. In addition, as the requirements of multiple features in the location-feature-position method are hard to achieve (described in Section 2.3), we cannot implement this approach for our research. We conducted simulation and analysis for these two approaches, which further demonstrate show their defects if being applied in this research. Motivated by problems of these two approaches, we aim to develop an approach to track the leader using only one camera and one feature.

The remainder of this chapter is organized as followers. Chapter 2.2 describes the projection model of a camera. Chapter 2.3 describes and evaluates the location-feature-area approach. Chapter 2.4 describes and evaluates the location-feature-position approach. Chapter 2.5 provides a brief conclusion and discusses a key assumption that we use for target' location tracking using camera vision.

2.2 Camera Projection Model

This section describes the camera projection model that is used to locate an object's position. This model represents the geometric relationship between an image point and its relative point in the camera coordinates. As shown in Figure 1.(a), O is the original point in the camera's coordinates; Z axis is the optical axis of the camera and perpendicular to the image plane at point o; o is the original point in the image coordinates; the distance between O and image plane is f, in fact, f is the camera's focal length; point P (X, Y, Z) in the camera coordinates projects to point p (x, y) on the image plane.

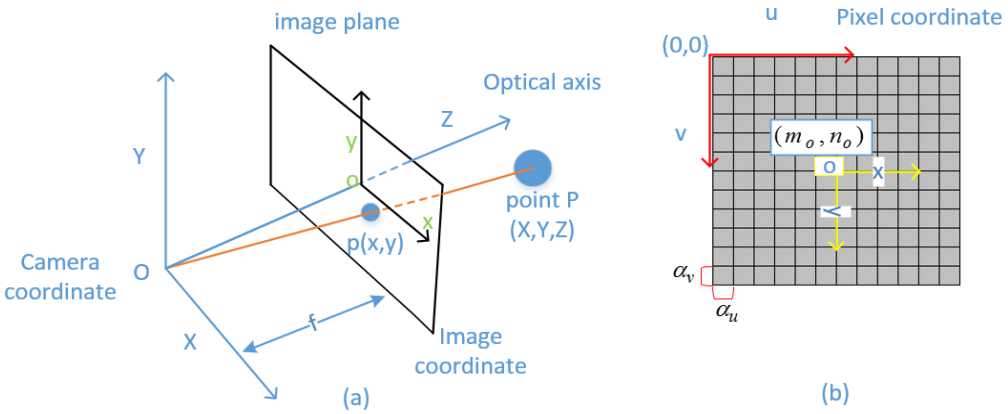

Figure 1 Illustration of camera projection; (a) The projection from the camera frame to the image plane. (b) The original point ***o*** of the image coordinates is the center point of the pixel coordinates.

According to book [9], point P projects to point p via:

$$\begin{bmatrix} x \\ y \\ 1 \end{bmatrix} = \begin{bmatrix} \frac{f}{z} & 0 & 0 \\ 0 & \frac{f}{z} & 0 \\ 0 & 0 & 1 \end{bmatrix} \begin{bmatrix} X \\ Y \\ 1 \end{bmatrix} \tag{2-1}$$

Then point p projects on the CCD (charged coupled device) sensor plane and it can be expressed in the pixel coordinate via:

$$\begin{bmatrix} m \\ n \\ 1 \end{bmatrix} = \begin{bmatrix} \frac{1}{\alpha_u} & 0 & m_o \\ 0 & \frac{1}{\alpha_v} & n_o \\ 0 & 0 & 1 \end{bmatrix} \begin{bmatrix} x \\ y \\ 1 \end{bmatrix} \tag{2-2}$$

where (m_o, n_o) is the principle point in pixel coordinate, α_u and α_v are one pixel physical dimensions in the horizontal direction u and vertical direction v (see Figure 1).

In view of (2-1) and (2-2), the above matrix is rewritten as:

$$\begin{bmatrix} m \\ n \\ 1 \end{bmatrix} = \begin{bmatrix} 1/\alpha_u & 0 & m_o \\ 0 & 1/\alpha_v & n_o \\ 0 & 0 & 1 \end{bmatrix} \begin{bmatrix} \frac{f}{z} & 0 & 0 \\ 0 & \frac{f}{z} & 0 \\ 0 & 0 & 1 \end{bmatrix} \begin{bmatrix} X \\ Y \\ 1 \end{bmatrix} \tag{2-3}$$

$$\begin{bmatrix} m \\ n \\ 1 \end{bmatrix} = \begin{bmatrix} \frac{f_x}{z} & 0 & m_o \\ 0 & \frac{f_y}{z} & n_o \\ 0 & 0 & 1 \end{bmatrix} \begin{bmatrix} X \\ Y \\ 1 \end{bmatrix} \tag{2-4}$$

where $f_x = f/\alpha_u,\ f_y = f/\alpha_v$. In addition, $f_x, f_y,\ m_o, n_o$ are the intrinsic parameters and can be obtained by the camera calibration procedure.

2.3 The Location-feature-area Method

The section reviews the location-feature-area method which was implemented on the CMUcam5 Pixy sensor (Pixy) [7] in Figure 2. This sensor was designed by Charmed Labs for color detection. It consists of a microcontroller NXP LPC4330 and an image sensor Omnivision OV9715. Pixy possesses the following features. 1) It has a fast speed to process digital images. Its speed can arrive 50 times per second. 2) It is convenient for users to use. Pixy has a friendly interface which works with Raspberry Pi, Arduino, and BeagleBone. Pixy provides its library for these microcontrollers so that users don't need to knowledge principles of pattern recognition or compile codes to detect a target. The detection procedure of Pixy is in the following. Through the software PixyMon that Charmed Labs offers, users decide which color to be identified. When the target color is detected, Pixy draws the target with a straight rectangle. For instance, in Figure 3, the target color is red, and the Pixy draws

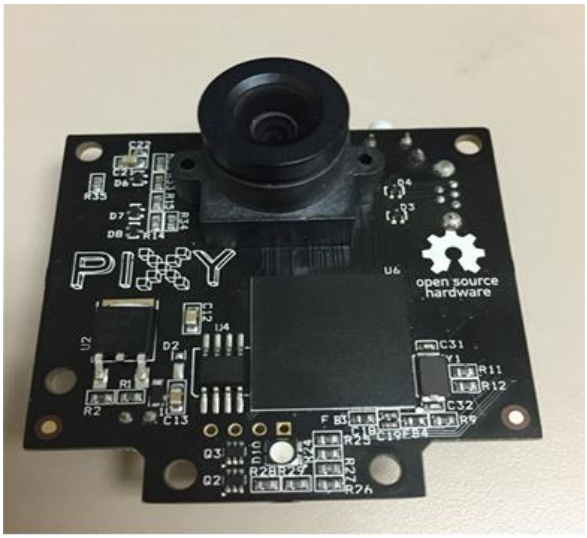

Figure 2 CMUcam5 Pixy sensor.

out the target with a square contour. Users just call functions from Pixy's library to obtain the area S and center location $(x_u(t), y_v(t))$ of the contour in the camera frame. Meanwhile, the bearing angle $\beta(t)$ between the camera and the heading of the robot can be obtained.

In paper [7], a mobile robot tracks a ball using a proportional controller:

$$V_F(t) = S_d - S(t)v_{gain}$$

$$\mathrm{d_v}(t) = ((\beta_d - \beta(t)) + (\beta_d - \beta(t))V_f(t)\,)d_{gain}$$

$$V_l(t) = V_F(t) + d_v(t)$$

$$V_r(t) = V_F(t) - d_v(t)$$

Where $S_d$is the desired size of the ball, β_d is the desired bearing angular, V_{gain} and d_{gain} are

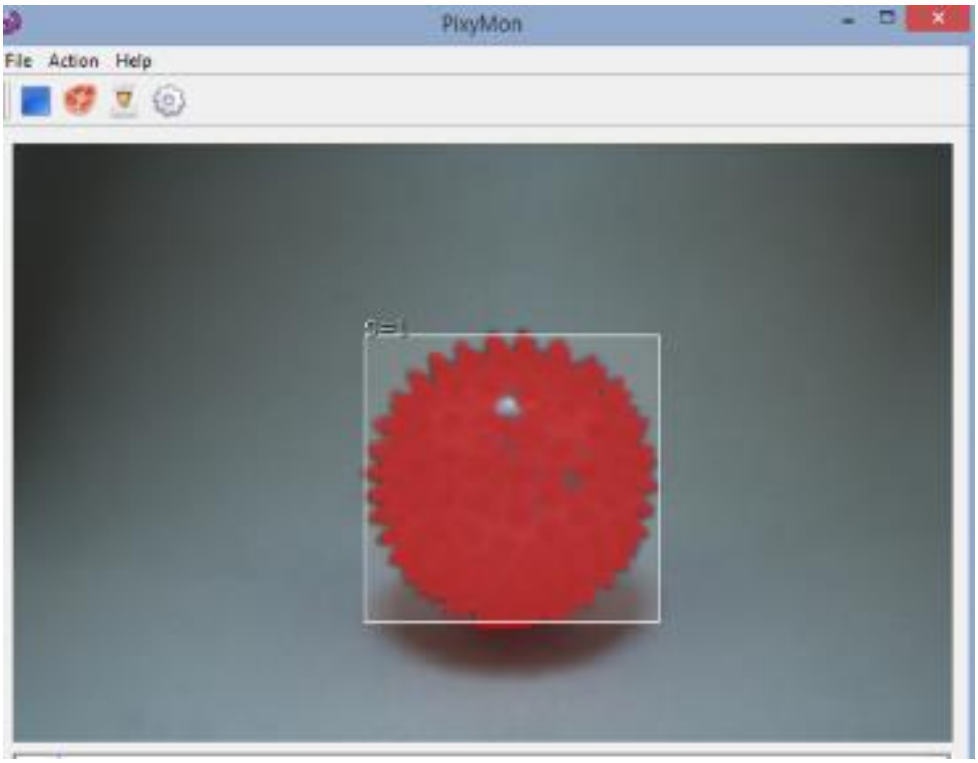

Figure 3 The contour of detected target (taken from [7]).

the feedback gains, $\mathrm{d_v}\,(t)$Steering differential, $V_l\,(t)$is the velocity of left wheel, $V_r(t)$ is the velocity of right wheel.

And the controller for the camera to tracking the ball is shown in the following equations

$$\mathrm{e_x}(t) = x_{u0} - x_u(t)$$

$$e_y(t) = y_u(t) - y_{uo}$$

$$V_{cp}(t) = e_x(t)pGain + \dot{e_x}(t)dGain$$

$$V_{ct}(t) = e_y(t)pGain + \dot{e_y}(t)dGain$$

where (x_{u0}, y_{v0}) is the intrinsic center of the camera, the derivatives of $e_x(t)$ and $e_y(t)$ are $\dot{e_x}$ and $\dot{e_y}$ $pGain$ and $dGain$ are the feedback gains, $V_{cp}(t)$ and $V_{ct}(t)$ are the velocities of the pan servo and the tilt servo. In order to simulate the leader-follower tracking system using the location-feature-area method, we build the code to simulate in MATLAB.

The pseudocode for leader-follower tracking system using the location-feature-area method	
Step 1:	Initialization
1.1	$\big(x_f(1), y_f(1)\big) = (50,25), V_f(1) = 0, W_f(1) = 0, \beta_d = 0,\ S_d = 400, (x_{u0}, y_{v0}) = (160,120)$ and the total time steps t_{total}=1000
1.2	**for** t =1: t_{total}
Step 2:	Object detection
2.1	According to the ball's projection in the pixel frame, one obtains S and (x_u, y_v)
Step 3:	Calculate the velocities of follower
3.1	**if** $S(t) = S_d$ && $\beta(t) = \beta_d$
3.2	$V_l(t) \leftarrow 0, V_r(t) \leftarrow 0$;
3.3	**else**
3.4	Calculate $V_F(t)$ and $d_v(t)$ with equation (2-6);
3.5	$V_l(t) \leftarrow V_F(t) + d_v(t)$;
3.6	$V_r(t) \leftarrow V_F(t) - d_v(t)$;
3.7	**end**
Step 4:	Update the position of the follower
4.1	$\beta(t+1) = \beta(t) + \frac{V_r - V_l}{b}\ \delta$; %$\delta$ is the sampling time, b is the distance between the centers of the left wheel and right wheel
4.2	$x_f(t+1) = x_f(t) + \frac{V_r + V_l}{2}\cos(\beta(t+1))\delta$;
4.3	$y_f(t+1) = y_f(t) + \frac{V_r + V_l}{2}\sin(\beta(t+1))\delta$;
Step 5:	Update the bearing angular $\beta(t+1)$
5.1	**if** $(x_u, y_v) = (x_{u0}, y_{v0})$
5.2	$V_{cp} \leftarrow 0, V_{ct} \leftarrow 0$;
5.3	**else**
5.4	$V_{cp} \leftarrow e_x pGain + \dot{e_x} dGain$;
5.5	$V_{ct} \leftarrow e_y pGain + \dot{e_y} dGain$;

5.6	**end**
5.7	$\beta(t+1) = \beta(t) + V_{cp}\delta$; go to back step 2
	end

The result of the simulation is shown in Figure 5. In order to simulate the real scenario, an arbitrary trajectory of the leader is created using the smooth-turn mobile model [10] in Figure 4 . The starting points of the leader target and follower robot are (51, 26) and (51, 25). As shown in Figures 4, 5, although the follower follows the ball to move, the follower cannot achieve the desired tracking performance. The bearing angle $\beta\ (t)$ is more than 0.5 in the last part of the simulatition. In the implementation of Pixy, some defects of location-feature-area are observed: 1) It cannot estimate the relative position between the camera and the leader ball, and such it cannot implement an advanced controller to improve the performance of leader-follower tracking proplem. 2) The camera cannot distinguish the detected target from objects with a similar color. As a result, the camera may lose the identified target easily. Sometimes,

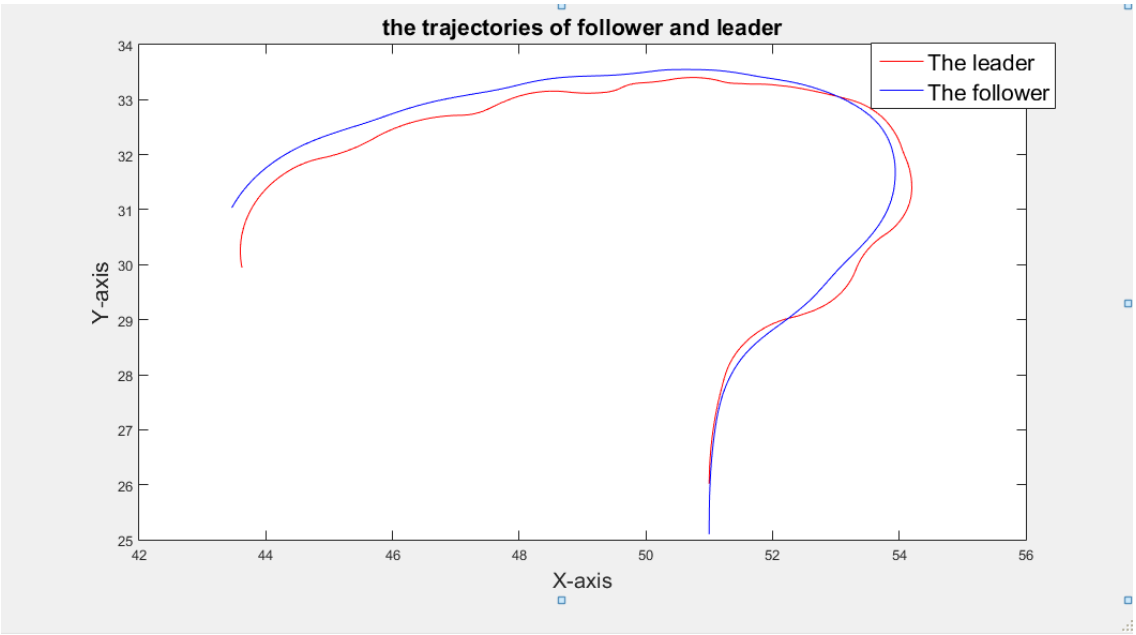

Figure 4 The trajectories of follower and leader. The follower tracks the leader using the location-feature-area method.

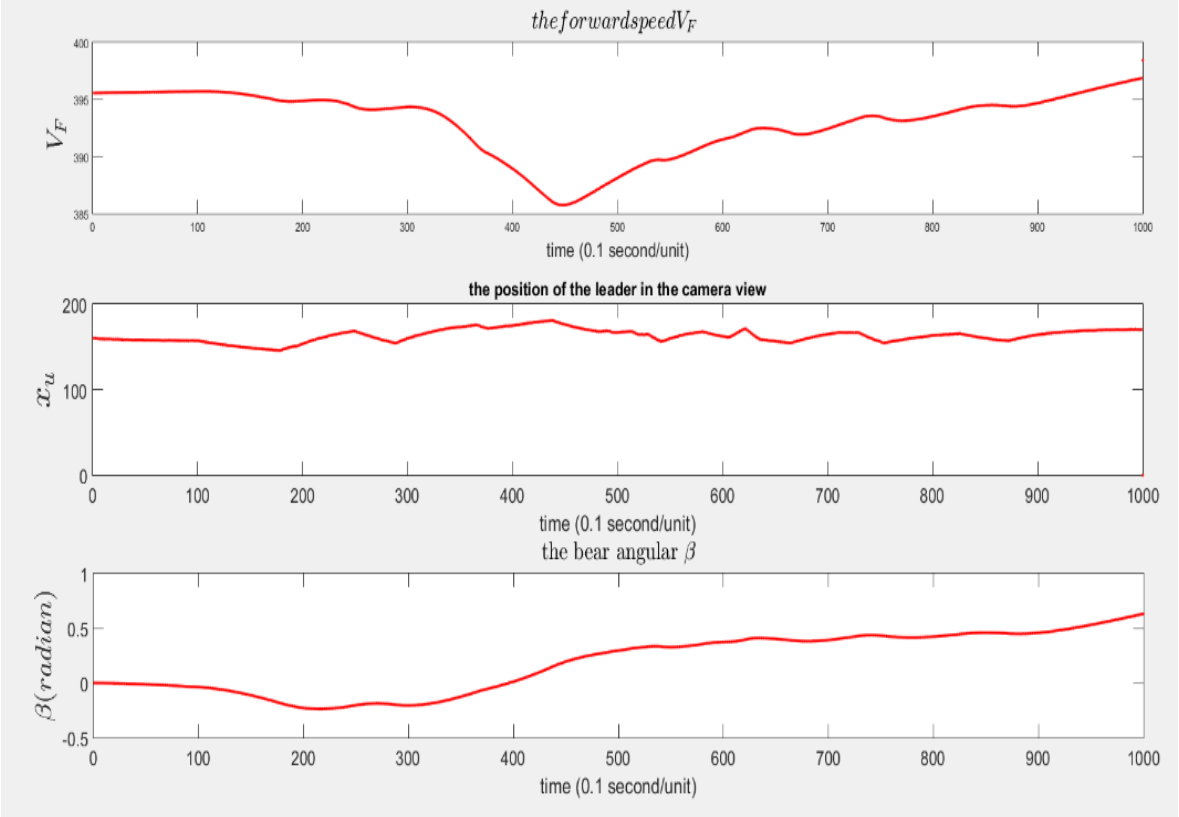

Figure 5 Simulation result. $\boldsymbol{V_F}$ is the follower's velocity. $\boldsymbol{x_u}$ is the position of the ball in the camera view. $\boldsymbol{\beta}$ is the beading angular between the camera and the heading of the robot.

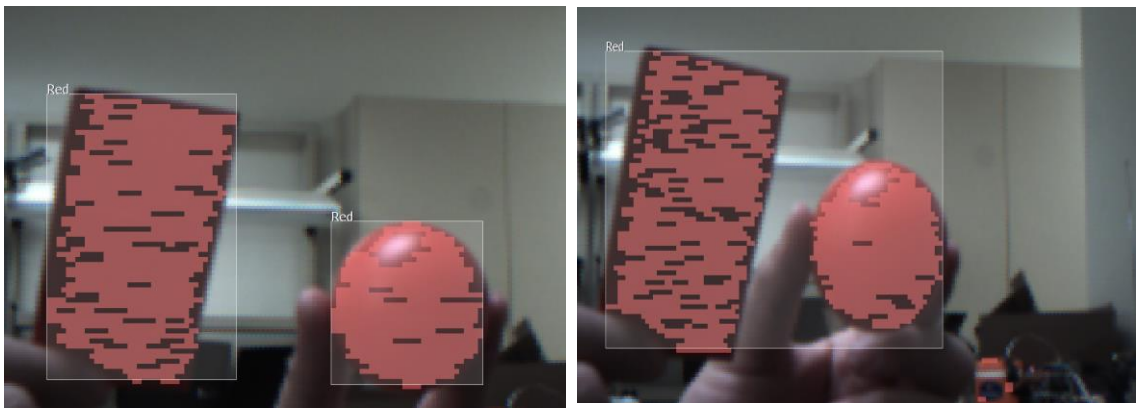

Figure 6 Target detection in Pixy. The ball is the detected target and the rectangle is noise. (a) The noise is identified as a target. (b) The ball and noise are identified as a target.

Pixy may draw the target with noise and then calculate the area of contour in a wrong way (see Figure 6). Due to these defects, this algorithm does not perform well.

2.4 The Location-Feature-Position Method

This section reviews and analyzes the location-feature-position method. In this algorithm [6], the altitudes of three features are not equal to zero in the camera coordinate, the height of one feature must be positive in the camera coordinate, and these features are not on one perpendicular plane of the follower robot's motion plane. Also, the camera must always detect three separate features. According to the camera projection model and geometric analysis between the leader, camera and the desired position of the follower [8], the following formation can calculate the bearing angular β between the headings of the follower robot and the leader target:

$$a_{ij}sin\Delta + b_{ij}cos\Delta = c_{ij} \tag{2-7}$$

where

$$\Delta = -\varphi + \varphi^* + \beta$$

$$a_{ij} = -x_i x_j^* - y_i y_j^* + y_j y_i^* + x_j x_i^*$$

$$b_{ij} = -x_i y_j^* + y_i x_j^* - y_j x_i^* + x_j y_i^*$$

$$c_{ij} = -x_i y_j + y_i x_j - x_i^* y_j^* + y_i^* x_j^* \tag{2-8}$$

φ is the bearing angular between the camera and the heading of the follower robot, φ^* is the desired bearing angular between the camera and the heading of the follower robot, $x_i = \frac{X_i}{Z_i}, y_i = \frac{Y_i}{Z_i}\ and\ (X_i, Y_i, Z_i)$ is the position of one feature Q_i in the camera frame, $x_i^* = X_i^*/Z_i^*, y_i^* = Y_i^*/Z_i^*$ and (X_i^*, Y_i^*, Z_i^*) is the desired position of the feature Q_i in the camera frame, $x_j = \frac{X_j}{Z_j}, y_i = \frac{Y_j}{Z_j}\ and\ (X_j, Y_j, Z_j)$ is the position of one feature Q_j in the camera frame, $x_j^* = X_j^*/Z_j^*, y_j^* = Y_j^*/Z_j^*$ and (X_j^*, Y_j^*, Z_j^*) is the desired position of the feature Q_j in the camera frame. When the number of features is 3, the following formation can be obtained from (2-1):

$$\begin{bmatrix} sin\Delta \\ cos\Delta \end{bmatrix} = (C^T C)^{-1} C^T D \tag{2-9}$$

where

$$C = \begin{bmatrix} a_{12} & b_{12} \\ a_{13} & b_{13} \\ a_{23} & b_{23} \end{bmatrix},\ D = \begin{bmatrix} c_{12} \\ c_{13} \\ c_{23} \end{bmatrix} \tag{2-10}$$

According to equation (2-3), the bearing angular β is

$$\beta = atan2(sin\Delta, cos\Delta) + \varphi - \varphi^* \tag{2-11}$$

As the camera cannot measure the location error (X_e, Y_e) between the current location and desired location of the follower robot, the paper [8] defines new variables $(\mathrm{x_e}, \mathrm{y_e}) = (X_e/Z_l, Y_e/Z_l)$ where Z_l is the altitude of one feature in the camera feature. $(\mathrm{x_e}, \mathrm{y_e})$ is measureable through the camera projection model. In the location-feature-position method, any one feature of the three features can be chosen as the position of the leader. The target feature is denoted as $Q_1(X_1, Y_1, Z_1)$. Through the geometric analysis [8], $(\mathrm{x_e}, \mathrm{y_e})$ is calculated by the following equation:

$$\begin{bmatrix} x_e \\ y_e \end{bmatrix} = R(\beta) \begin{bmatrix} x_d \\ y_d \end{bmatrix} + R(\varphi) \begin{bmatrix} x_1 \\ y_1 \end{bmatrix} \tag{2-12}$$

where $x_d = \frac{X_d}{Z_1}$, $y_d = \frac{Y_d}{Z_1}$ and (X_d, Y_d) is the desired position of the follower corresponding to the leader; $x_1 = \frac{X_1}{Z_1}, y_1 = \frac{Y_1}{Z_1}$; $R()$ is a rotation matrix: $\begin{bmatrix} \cos() & -\sin() \\ \sin() & \cos() \end{bmatrix}$. The procedure of the leader-follower tracking system using the location-feature-position method is shown in Figure 7. In this procedure, v_f is the velocity of the follower, w_f is the angular velocity of the follower, (X_f, Y_f) is the position of the follower in the world coordinates, w_c is the angular velocity of the camera, and e_x is the error between the current position and the desired position of Q_1 at the horizontal direction in the pixel coordinates. The follower controller $f(x_e, y_e, \beta)$ and pan camera controller $C(e_x, w_f)$ are backstepping controller which builds a stabilizing controllers by a recursive method.

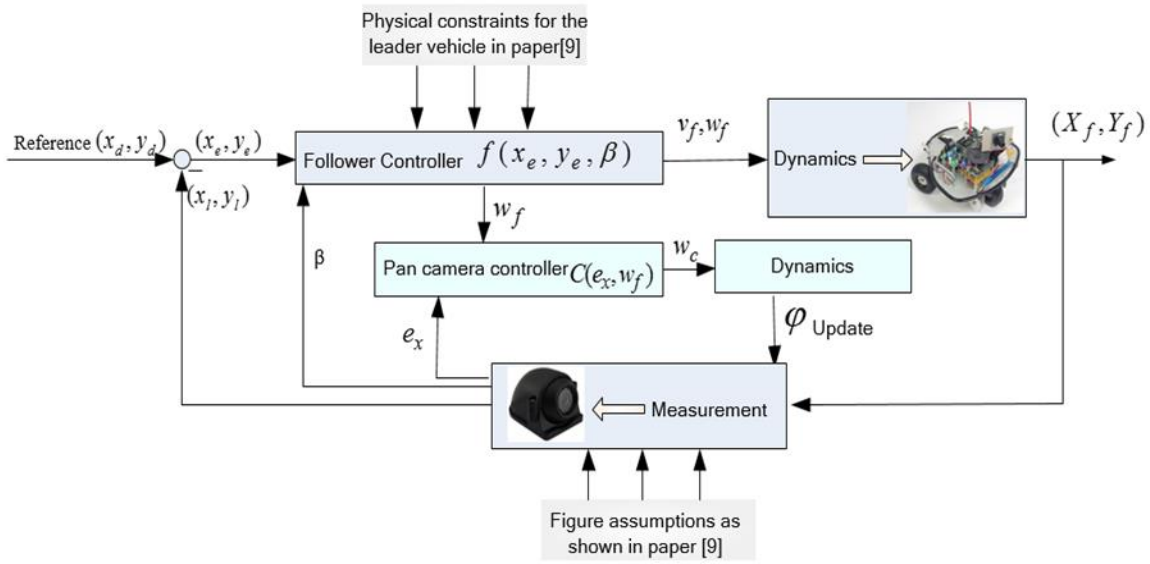

Figure 7 The diagram of the leader-follower tracking system using the location-feature-position method.

In order to simulate the leader-follower tracking system using the location-feature-position method, we build the following codes to simulate in MATLAB.

Step 1:	Initialization
1.1	$X_d = 0.5, Y_d = 0.3, v_f = 0, w_f = 0, X_f = 49.50, y_f = 24, m_1^* = 419.299$, the total time steps $t_{total} = 1000$, $\varphi^* = \frac{\pi}{6}$, ; the orientation angular of the follower $f_d = pi/2$ Note: m_1^* is the desired position of the feature Q_1in the pixel coordinates;
	for t =1: t_{total}
Step 2:	Object detection
2.1	$\beta \leftarrow atan2(sin\Delta, cos\Delta) + \varphi - \varphi^*$
2.2	$\begin{bmatrix} x_e \\ y_e \end{bmatrix} \leftarrow R(\beta) \begin{bmatrix} x_d \\ y_d \end{bmatrix} + R(\varphi) \begin{bmatrix} x_1 \\ y_1 \end{bmatrix}$
2.3	$e_x \leftarrow m_1 - m_1^*$; % m_1 is the position of feature Q_1 at the horizontal direction of the pixel coordinates.
Step 3:	Update the position of the follower
3.1	$v_f, w_f \leftarrow f(x_e, y_e, \beta)$;
3.2	$f_d \leftarrow f_{dpre} + w_f \delta$; %δ is the sampling time and $\delta = 0.1s$, f_{dpre} is the f_d at the last step time.
3.3	$X_f \leftarrow X_{fpre} + \mathrm{v}_f \cos(f_d)\delta$; % X_{fpre} is the X_f at the last step time;
3.4	$Y_f \leftarrow Y_{fpre} + \mathrm{v}_f \sin(f_d)\delta$; % Y_{fpre} is the Y_f at the last step time;
Step 4:	Update the bearing angular φ
4.1	$w_c \leftarrow C(e_x, w_f)$
4.2	$\varphi \leftarrow \varphi_{pre} + w_c \delta$; % φ_{pre} is the φ at the last step time;
4.3	Go back **step 2**
	end

As shown in Figures 8 and 9, the errors x_e, y_e tend to become zero, and the follower robot tracks the leader target well. To compare it with the location-feature-area method, the location-feature-position method can measure the bearing angular β and the relative position error (x_e, y_e). Furthermore, the follower robot can track the leader target by a relative position(x_d, y_d). In addition, an advanced controller for the leader-follower tracking system is built using the bearing angle β and position error(x_e, y_e).

In consideration of the requirements of features, three feature were used on the leader robot. If these features are small ones, the camera on the drone cannot catch them. If the features are large ones, they become close to each other and hence the camera cannot distinguish them as three separate features. Moreover, when we implement this method on a drone and a robot, it is possible that the height of one feature is zero in the camera frame. In this case, the camera cannot measure the position of the leader. As such, it's difficult to implement the leader-follower tracking system using the method location-feature-position for our drone-robot tracking problem.

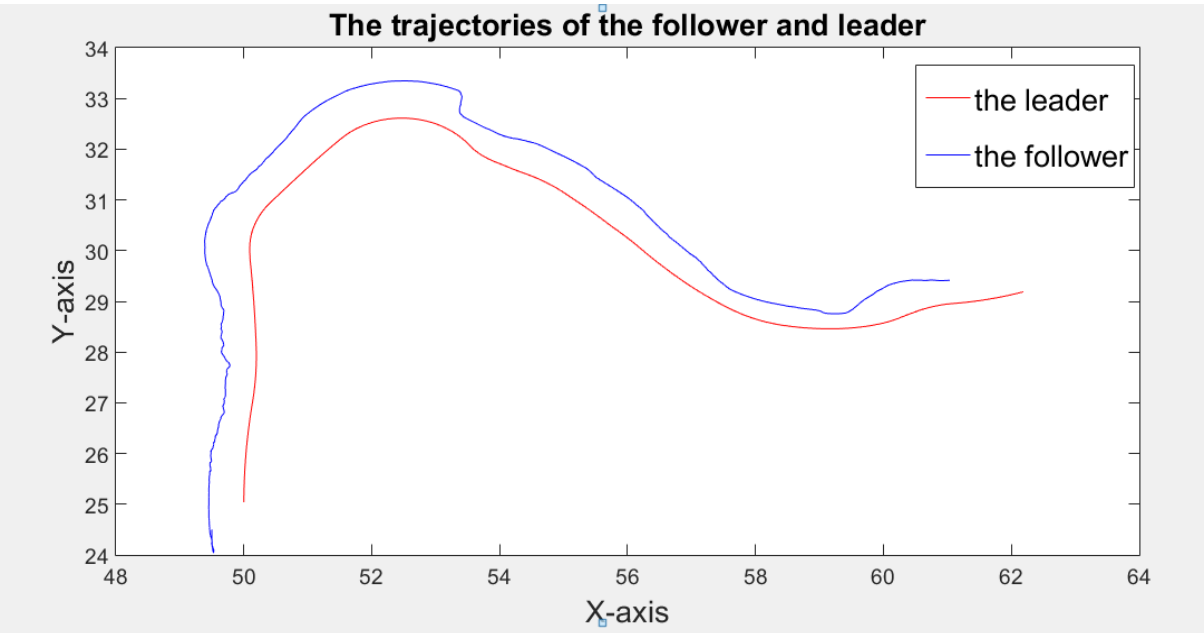

Figure 8 Trajectories of the follower and leader.

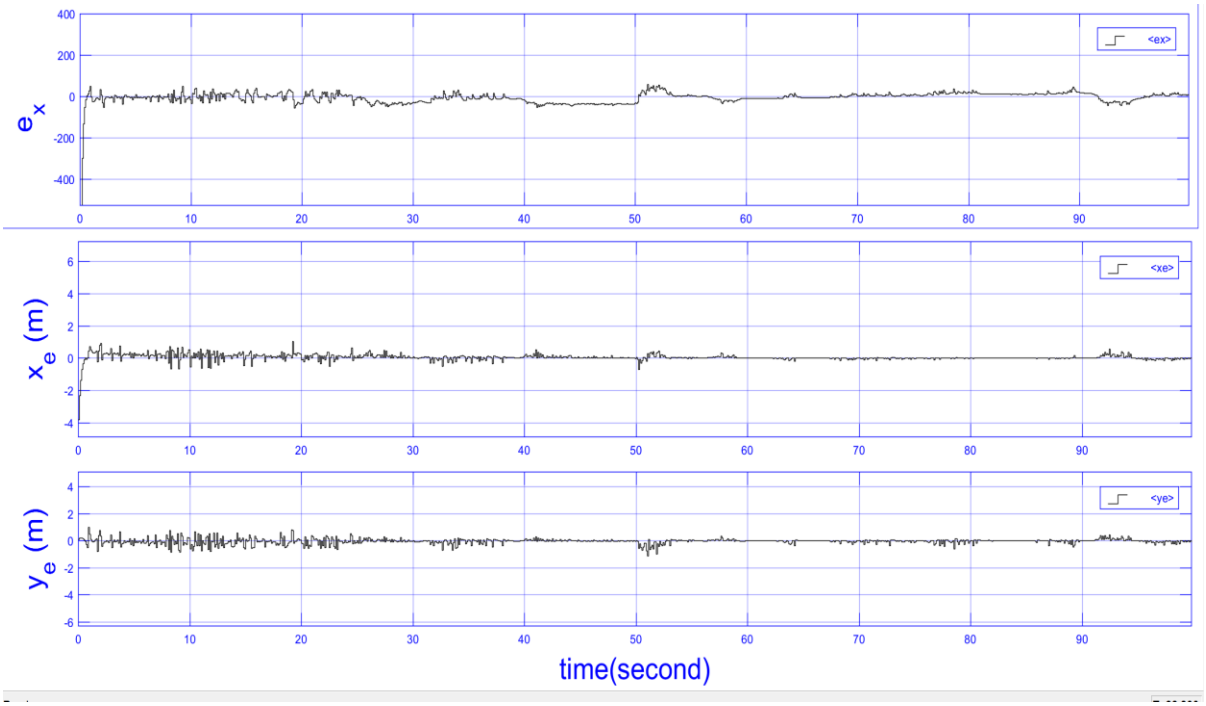

Figure 9 Simulation result. $\boldsymbol{e_x}$ is the image error. $\boldsymbol{x_e}$ and $\boldsymbol{y_e}$ are the formation error.

2.5 Conclusions

The location-feature-area method uses the area of one ball and the bearing angle β to scale the leader target's location in the camera frame to address the leader-follower trcking problem. However, the relative position of the follower and leader cannot be obtained. The location-feature-position method uses three features to calculate the target's relative position. Due to the requirement of three features, it is still unrealistic to implement in our research. Therefore, it is necessary to find a new effective approach to tracking using camera vision. The method can provide the accurate relative position of a detected object corresponding to the camera. Meanwhile, the approach only needs to use one camera and one feature. In this thesis, we use one camera and one feature to locate the target and then build a controller to address the leader- follower tracking problem. In Chapter 3, we describe how to locate a target using one camera and one ball.

CHAPTER 3

LEADER-FOLLOWER TRACKING ALGORITHM BASED ON A SINGLE SPHERE FEATURE

3.1 Introduction

In this section, we build a leader-follower tracking system with one camera installed on the follower and one sphere placed on the leader. In this tracking system, the leader's position need to be measured using a leader-follower tracking algorithm. Through the camera measurement and the geometry analysis between the follower and the leader, we can obtain the leader's location. Based on the estimated leader's position, we can build a control system on the follower to track the leader. As shown in Figure 10, we expect the follower to track the leader with the distance L and bearing angular λ. L is the distance between the camera's center O_l and the sphere's center O_c. λ is the bearing angular between the heading of the follower and $O_c O_l$. In order to keep the feature in the camera view, we also build a P-controller for a pan camera which just moves on its pan direction.

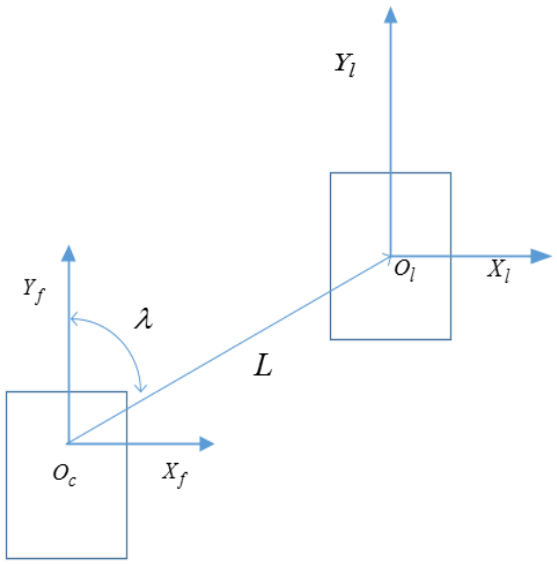

Figure 10 The formation of leading-follower tracking.

In this section, we first show how to use one camera to measure the sphere's relative position with respect to the follower and calculate the bearing angle β between the directions of the follower and the leader. Then, we build P-controllers that allow the follower to track the leader based on parameters that the camera measures.

3.2 Estimation of Sphere's Position in the Camera Coordinate System

In this section, we focus on the procedure to measure the leader's position using the camera vision in the camera's coordinates. First, we show the projection of a sphere on the image plane. Then we briefly describe the relationship between the image coordinate and the camera coordinate and introduce the procedures to transfer the sphere's location from the image coordinate to the camera coordinate.

3.2.1 Projection of a Sphere on the Image Plane

Figure 11 shows the projection of a sphere on the image plane, as marked in yellow. In fact, the projection is an ellipse which is the intersection plane of the image plane and the green cone. In this figure, O_s is the sphere's center with location (X_s, Y_s, Z_s) in the camera's coordinate. R_s is the radius of the sphere, and γ is the bearing angle between the vector $O_c O_s$ and the principal axis X_c, where O_c is the optical center.

As shown in Figure 10, the outline of the sphere's projection (yellow ellipse) is the projection of the green circle, which is the intersection of the sphere and the green cone tangent to the sphere. In paper [11], the ellipse is expressed by the following function:

$$\left(\frac{x}{a}\right)^2 + \left(\frac{y}{b}\right)^2 = 1 \tag{3-1}$$

Where $a \approx \frac{Z_s}{R_s}$, $b \approx \frac{Z_s}{R_s}\cos(\delta)$. The area A of the ellipse is $A = \pi ab$.

Next, let us show the calculation of the sphere's center location (X_s, Y_s, Z_s).

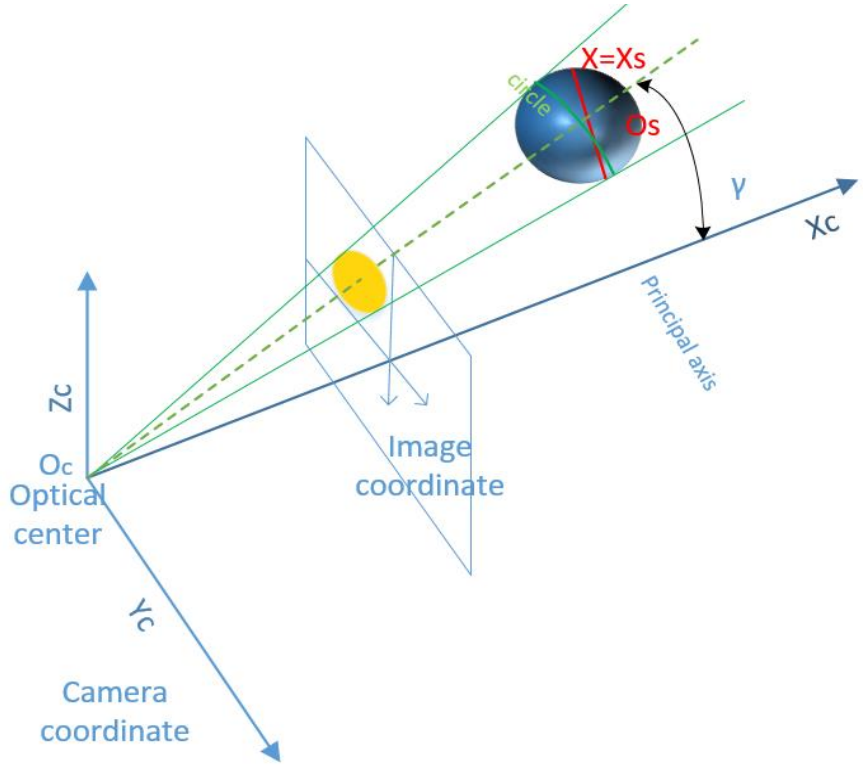

Figure 11 Projection of a sphere on the image plane.

3.2.2 Relationship between the Image Coordinates and the Camera Coordinates

Suppose (m_i, n_i) is the location of a point in the image coordinate, then it has the following relationship with its corresponding location (X_i, Y_i, Z_i) in the camera coordinate $X_c Y_c Z_c$ (see the Figure 11), according to the camera projection model:

$$m_i = f_y \frac{Y_i}{X_i} + m_o \tag{3-2}$$

$$n_i = f_z \frac{Z_i}{X_i} + n_o \tag{3-3}$$

Where $f_y = f/\alpha_u$ and $f_z = f/\alpha_v$, f is the focal length, α_u, α_v are the pixel dimensions, and (m_o, n_o) is the location of the principal point of the camera in the image coordinates.

3.2.3 Estimation of the Sphere Position from an Image

The procedures introduced in paper [11] estimates the location of sphere's center (X_s, Y_s, Z_s) in the camera coordinates are shown as follows.

1) Estimate the center of the sphere's projection(m_s, n_s), and its area A.

2) According to equations 3-2,3-3, it's easy to obtain

$$\frac{Y_s}{X_s} = \frac{\mathrm{m_s - m_o}}{f_y} \tag{3-4}$$

$$\frac{Z_s}{X_s} = \frac{n_s - n_o}{f_z} \tag{3-5}$$

3) Denote $\frac{Y_s}{X_s}$ as y_s, and $\frac{Z_s}{X_s}$ as z_s, then the bearing angle $\gamma = -arctan\sqrt{y_s^2 + z_s^2}$.

4) Calculate the area A of the sphere' ellipse projection by $A = N/(f_Y f_z)$, where N is the number of pixels in this area.

5) Compute $X_s = R_s\sqrt{\pi/(A cos\gamma)}$. Then $Y_s = y_s X_s$, $Z_s = z_s X_s$.

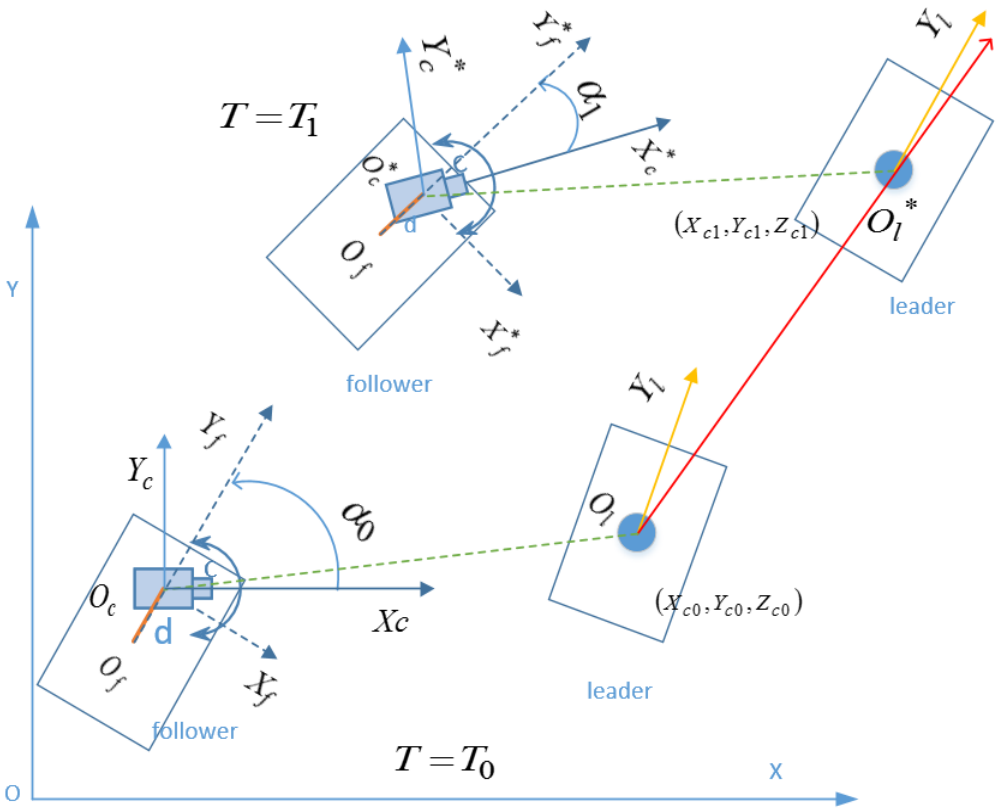

Figure 12 Leader-follower formation.

Table 1 Definitions of Notations used in Figure 12

Y_l	the heading of the leader
Y_f, Y_f^*	the heading of the follower at T_0, T_1
O_f	the center of the follower
O_c,O_C^*	the optical center of the camera
d	the distance between O_f and O_c
O_l	the center of the leader at T_0
O_l^*	the center of the leader at T_1
OXY	The world coordinates
$O_cX_fY_f$	robot frame of the follower at T_0
$O_c^*X_f^*Y_f^*$	robot frame of the follower at T_1
$O_cX_cY_c$	camera frame at T_0
$O_c^*X_c^*Y_c^*$	camera frame at T_1
α_0 , α_1	the orientation of the camera corresponding to the follower at time T_0 and T_1
O_lY_l	the direction of the leader
$O_lO_l^*$	Direction vector of the leader's motion
X_{c0}, Y_{co}, Z_{c0}	the camera coordinate of $O_l$at T_0
X_{c1}, Y_{c1}, Z_{c1}	the camera coordinate of O_l^*at T_1

3.3 Estimation the Bearing Angle β and the Relative Position of the Sphere

In this section, we introduce the process to estimate the bearing angle β and the relative position of the sphere in the follower's coordinates. In order to measure β, we need to measure the relative position of the sphere and transfer the positions of the sphere at time T_1 and T_0 into the follower's coordinate $O_c^*X_f^*Y_f^*$ (see Figure 12).

3.3.1Transfer Sphere's Position at Time T_0 to the Follower's Coordinates $O_c^*X_f^*Y_f^*$

In this section, we show the transformation of the sphere's location from the image coordinates to the follower's coordinate $O_c^*X_f^*Y_f^*$ at T_0. Denote the location of the sphere and its area obtained by the camera at time T_0 as (m_{t0}, n_{t0}) and A_0, respectively. According to Section 3.2, we can get the sphere's center location (X_{c0}, Y_{c0}, Z_{c0}) in the camera coordinates.

In order to transfer (X_{c0}, Y_{c0}) to the coordinate $O_c^* X_f^* Y_f^*$, we first need to transfer it to the coordinate $O_c X_f Y_f$. This can be realized through coordinate space transformation as follows.

$$\begin{bmatrix} X'_{c0} \\ Y'_{c0} \end{bmatrix} = R(\pi/2 - \alpha_0) \begin{bmatrix} X_{c0} \\ Y_{c0} \end{bmatrix}$$

Where α_0 is the bearing angle among X_c and the direction Y_f at time T_0, (X'_{c0}, Y'_{c0}) is the location of the sphere's center in $O_c X_f Y_f$. R is the rotation matrix shown as follows

$$R(\cdot) = \begin{bmatrix} \cos(\cdot) & -\sin(\cdot) \\ \sin(\cdot) & \cos(\cdot) \end{bmatrix} \tag{3-7}$$

Now we can calculate the location of the sphere's center in the coordinate $O_c^* X_f^* Y_f^*$. In order to achieve this, we first need to obtain the moving direction of the follower from T_0 to T_1, which is approximated as the direction of the vector $O_c O_c^*$ in OXY (see Figure 12). Suppose the velocity and angle velocity of the follower are v and w, which can be obtained by encoders. The direction angular of the follower in OXY is θ. Then, $O_c O_c^* = (\Delta x, \Delta y)$ can be obtained by following equations

$$\Delta x = (v\cos(\theta + w\Delta T) + dw\cos(\theta + w\Delta T)) \cdot \Delta T \tag{3-8}$$

$$\Delta y = (v\sin(\theta + w\Delta T) + dw\sin(\theta + w\Delta T)) \cdot \Delta T \tag{3-9}$$

where $\Delta T = T_1 - T_0$ and d is the distance between the center of the follower and the camera. Then we can get the location (X_0, Y_0) of sphere's center O_l in the coordinate $O_c^* X_F^* Y_f^*$ as follows

$$\begin{bmatrix} \mathrm{X}_0 \\ \mathrm{Y}_0 \end{bmatrix} = \mathrm{R}(\pi/2 - \alpha_0 - w\Delta T) \begin{bmatrix} \mathrm{X}_{c0} \\ \mathrm{Y}_{c0} \end{bmatrix} - \mathrm{R}(\pi/2 - \theta - w\Delta T) \begin{bmatrix} \Delta x \\ \Delta y \end{bmatrix} \tag{3-10}$$

3.3.2 Transfer Sphere's Location at Time T_1 To The Follower's Coordinate $O_c^* X_f^* Y_f^*$

In this section, we introduce the transformation of the sphere's location O_l from the image coordinate to the follower's coordinate $O_c^* X_f^* Y_f^*$. Denoting the position of the sphere and its area obtained by the camera at time T_1 as (m_{t1}, n_{t1}) and A_1 respectively, we can follow the procedures introduced in Section 3 to calculate the sphere's center location (X_{c1}, Y_{c1}, Z_{c1}). Then the sphere's center location in the follower's coordinate $O_c^* X_f^* Y_f^*$, denoted as (X_1, Y_1), can be

obtained through simple coordinate space transformation. The mathematical equation is shown as follows.

$$\begin{bmatrix} \mathrm{X}_1 \\ \mathrm{Y}_1 \end{bmatrix} = \mathrm{R}(\pi/2 - \alpha_1) \begin{bmatrix} \mathrm{X}_{c1} \\ \mathrm{Y}_{c1} \end{bmatrix} \tag{3-11}$$

where α_1 is the bearing angle between axes X_c^* and Y_f^* at timeT_1 (see Figure 12).

3.3.3 Estimation of the Bearing Angle β

Having obtained the location of the sphere expressed in the follower's coordinate $O_c^* X_f^* Y_f^*$ at T_0 and T_1, we can now calculate the bearing angle β between the follower's direction Y_f^* and the motion vector $O_l O_l^*$ of the leader, using the following equation:

$$\beta = \begin{cases} \arctan\left(\frac{X_1 - X_0}{Y_1 - Y_0}\right) & if\ Y_1 - Y_0 > 0 \\ \arctan\left(\frac{X_1 - X_0}{Y_1 - Y_0}\right) + \pi & if\ Y_1 - Y_0 < 0 \text{ and } X_1 - X_0 \geq 0 \\ \arctan\left(\frac{X_1 - X_0}{Y_1 - Y_0}\right) - \pi & if\ Y_1 - Y_0 < 0 \text{ and } X_1 - X_0 < 0 \\ +\frac{\pi}{2} & if\ Y_1 - Y_0 = 0 \text{ and } X_1 - X_0 > 0 \\ -\frac{\pi}{2} & if\ Y_1 - Y_0 = 0 \text{ and } X_1 - X_0 < 0 \\ 0 & if\ Y_1 - Y_0 = 0 \text{ and } X_1 - X_0 > 0 \end{cases} \tag{3-12}$$

3.4 Controller Design

In this section, we design P-controllers for the leader-follower tracking system using camera vision. As shown in Figure 12, we expect the follower tracks the leader with the distance L and bearing angular λ. L is the distance between the camera's center O_l and the sphere's center $\mathrm{O_c}$. λ is the bearing angular between the heading of the follower and $\mathrm{O_c}O_l$. In the process of leader -follower tracking system, the follower need to adjust its velocity v_f and angular velocity w_f to keep itself at the desired position corresponding to the leader. The driver model of the robot can influence how to adjust v_f and w_f so that it is necessary to comprehend the kinematics of the follower robot. In this project, we apply the controller algorithm on a

differential driver robot with DC motors. Therefore, Section 3.4.1 introduces the differential drive kinematics and DC motor model. Then, Section 3.4.2 focuses on the P-controller design.

3.4.1 The Differential Drive Kinematics and DC Motor Model

The differential drive kinematics model [13] is:

$$w(t) = \frac{v_r(t) - v_l(t)}{b} \tag{3-13}$$

$$v(t) = \frac{v_r(t) + v_l(t)}{2} \tag{3-14}$$

where $w(t)$ is the angular velocity of the robot, $v(t)$ is the velocity of the robot, $v_r(t)$ and $v_l(t)$ are the velocity of the wheel at the right side and left side, b is the distance from the left-side wheel to the right-side wheel. According to Equations 3-13 and 3-14, we can obtain the following equations:

$$v_r(t) = \frac{2v(t) + bw(t)}{2} \tag{3-15}$$

$$v_l(t) = \frac{2v(t) - bw(t)}{2} \tag{3-16}$$

Assuming the radius of the wheel is R, we can get the angular velocity of the wheels are:

$$w_r(t) = \frac{v_r(t)}{R} \tag{3-17}$$

$$w_l(t) = \frac{v_l(t)}{R} \tag{3-18}$$

where $w_r(t)$ is the angular velocity of the wheel at the right side, $w_l(t)$ is the angular velocity of the right side.

The DC motor model [14] is

$$v_m = e + R_a i_a + L_a \frac{di_a}{dt} \tag{3-19}$$

$$J \frac{dw_m}{dt} + B_l w_m = T_e - T_l \tag{3-20}$$

$$T_e = K_b i_a \tag{3-21}$$

where v_m is the input voltage of the motor, e is the induced emf, R_a is the resistance of the motor, i_a is the current of the motor, $L_a$is a self –inductance, w_m is the motor's angular speed,

J is the inertia moment of the motor, B_l is the viscous friction coefficient, T_e is the air gap torque of the motor, T_l is the lode toque, K_b is the induced emf constant. To transform equation (3-19, 3-20) into their Laplace equations, we can get the following equations

$$I_a(s) = \frac{V_m(s) - K_b w_m(s)}{R_a + sL_a} \tag{3-22}$$

$$w_m(s) = \frac{K_b I_a(s) - T_l(s)}{(B_l + sJ)} \tag{3-23}$$

Formulations 3-22 and 3-23 indicate that the voltage of motor can control the angular velocity of a wheel. In fact, PWM (pulse-width modulation) is often used to adjust the voltage of a motor. Therefore, we can use the value of PWM to control the angular velocity of a motor. Since the angular velocity w_l, w_f decide the velocity and direction of the follower, we can control the value of PWM to control the follower's movement.

3.4.2 Control Design for the Follower and Camera

Our goal is that the follower tracks the leader with the desired bearing λ_d and desired length L_d. According to function 3-11, the camera measures the sphere's position $(X(k), Y(k))$ at time k in the follower's coordinate. The distance $L(k)$ between the camera and the sphere is:

$$L(k) = \sqrt[2]{X^2(k) + Y^2(k)} \tag{3-24}$$

The bearing angular $\lambda(k)$ between the heading of the follower and the camera's direction is:

$$\lambda(k) = atan2(X(k), Y(k)) \tag{3-25}$$

Setting the setpoint (L_d, λ_d), we can build a P-controller algorithm for leader-follower tracking system:

$$v_f(k) = vgain(L(k) - L_d) \tag{3-26}$$

$$w_f(k) = wgain(\lambda_d - \lambda(k)) \tag{3-27}$$

where $vgain$ and $wgain$ are the gain of the P-controller. According to Equations from 3-13 to 3-18, we obtain the desired angular velocities $w_r(k), w_l(k)$ of the follower's wheels. The

current angular velocities $w_{rc}(k), w_{lc}(k)$ are measured by encoders installed on the shaft of the motors. Likewise, we design a new P control based on the error between w_r, w_l and w_{rc}, w_{lc} in order to make the rotational speeds of motors keep pace with their desired rotational speeds. The P-controller algorithm for motors is:

$$pwm_r(k) = p_{rgain}(w_r(k) - w_{rc}(k)) \tag{3-28}$$

$$pwm_l(k) = p_{lgain}(w_l(k) - w_{lc}(k)) \tag{3-29}$$

where p_{rgain} and p_{lgain} are the gains of the P-controller. Then we obtain the input PWM of the motors:

$$PWM_r(k) = PWM_r(k-1) + pwm_r\ (k) \tag{3-30}$$

$$PWM_l(k) = PWM_l(k-1) + pwm_l\ (k) \tag{3-31}$$

where PWM_r and PWM_l are the input PWMs of motors at the time k, $PWM_r\ (k-1)$ and $PWM_l(k-1)$ are the input PWM of motors at the time $k-1$. In the whole process of leader-follower tracking system, the camera needs to track the sphere on the leader and keep the ball in the camera view. Otherwise, the camera will lose the target and cannot estimate the relative position of the leader. As a result, it is necessary to build a controller to make the camera keep pace with the ball's movement. We also build a P-controller algorithm for the camera which moves on its pan direction. The desired position of the ball is the center point of the camera view in the pixel coordinates. Denote the center point of the camera view is m_o at the pan direction of the camera. The P-control of the camera is designed as follows:

$$w_c(k) = cgain(m_o - m(k)) \tag{3-32}$$

where $cgain$ is the feedback gain, $m(k)$ is the position of the ball in the camera frame at the time k, and $w_c(k)$ is the angular velocity of the camera.

3.5 Conclusion

In this chapter, we apply one camera and one ball to locate the leader's position corresponding with the follower. Meanwhile, through transferring the positions of the leader

into the follower's coordinates, we obtain the bearing angular β between the headings of the follower and leader. Then, we apply the information from the camera to build P-controllers for the leader-follower tracking system. In the next chapter, we focus on the simulation and implementation for leader-follower tracking system using camera vision.

CHAPTER 4

SIMULATION AND IMPLEMENTATION

In this section, we focus on the simulation and implementation of the leader-follower tracking system using camera vision. This section is organized as follows. Chapter 4.1 includes the procedure and results of simulation studies using MATLAB. Chapter 4.2 includes the hardware and software designs utilized in this research. Chapter 4.3 describe the procedure to detect an object using a Pi camera. Chapter 4.4 includes the procedure and results of the implementation for the leader-following tracking system.

4.1 Simulation

According to Chapter 3, we design a diagram in Appendix 1 to achieve the leader-following tracking task using one camera and one ball. In this figure, (x_f, y_f) is the position of the follower, $e_L = L_d - L(k)$, and $e_\lambda = \lambda_d - \lambda(k)$. Furthermore, to simulate the leader-follower tracking system using one camera and one ball, we build the following codes to simulate in MATLAB.

Step1:	Initialization
1.1	$L_d = 1.414\,m, \lambda_d = 0.7\,radian, m_0 = 243.942, n_o = 158.441$ $f_y = 497.157, f_z = 498.684, R_s = 0.06\,m\,, v_f(1) = 0, w_f(1) = 0,$ $PWM_l(1) = 0, PWM_r(1) = 0, x_f(1) = 50, y_f(1) = 25$, *total* =1000 $\varphi(1) = 0\,, \theta(1) = \pi/2;$ Note: R is the radium of the ball;
1.2	For $k = 1 : total$
Step 2:	Object detection
2.1	The camera obtains the position (m, n) of the ball in the pixel coordinate;
2.2	The camera measures the ball's position (X_{c0}, Y_{c0}, Z_{c0}) in the camera Coordinates
2.3	$\begin{bmatrix} X(K) \\ Y(K) \end{bmatrix} R(\pi/2 - \varphi(k)) \begin{bmatrix} X_{c0} \\ Y_{c0} \end{bmatrix}$
2.4	$L(k) \leftarrow \sqrt[2]{X^2(k) + Y^2(k)}$ $\lambda(k) \leftarrow atan2(X(k), Y(k))$
Step 3:	Calculate the velocity and angular velocity of the follower
3.1	$e_L \leftarrow L_d - L(k)$ $e_\lambda \leftarrow \lambda_d - \lambda(k)$

3.2	Through P-controller for the follower, calculate v_f, w_f
Step 4:	Update the position of the follower
4.1	$\theta(k+1) = \theta(k) + w_f\delta$; % δ is the sampling time
4.2	$x_f(k+1) \leftarrow x_f(k) + \mathrm{v}_f\cos(\theta(k+1))\delta$;
4.3	$y_f(k+1) \leftarrow y_f(k) + \mathrm{v}_f\sin(\theta(k+1))\delta$;
Step 5:	Update the bearing angular φ
5.1	$e_m \leftarrow m_o - m$
5.2	$w_c \leftarrow e_m cgian$
5.3	$\varphi(k+1) \leftarrow \varphi(k) + w_c\delta$;
5.4	Go back **step 2**
	end

As shown in Figure 13, the follower tracked the leader to move. In this simulation, the trajectory of the leader robot is created by the smooth-turn model [10]. The initial position and heading angle of the follower robot are $(50,25)$ and $\pi/2$. The initial position and heading angle

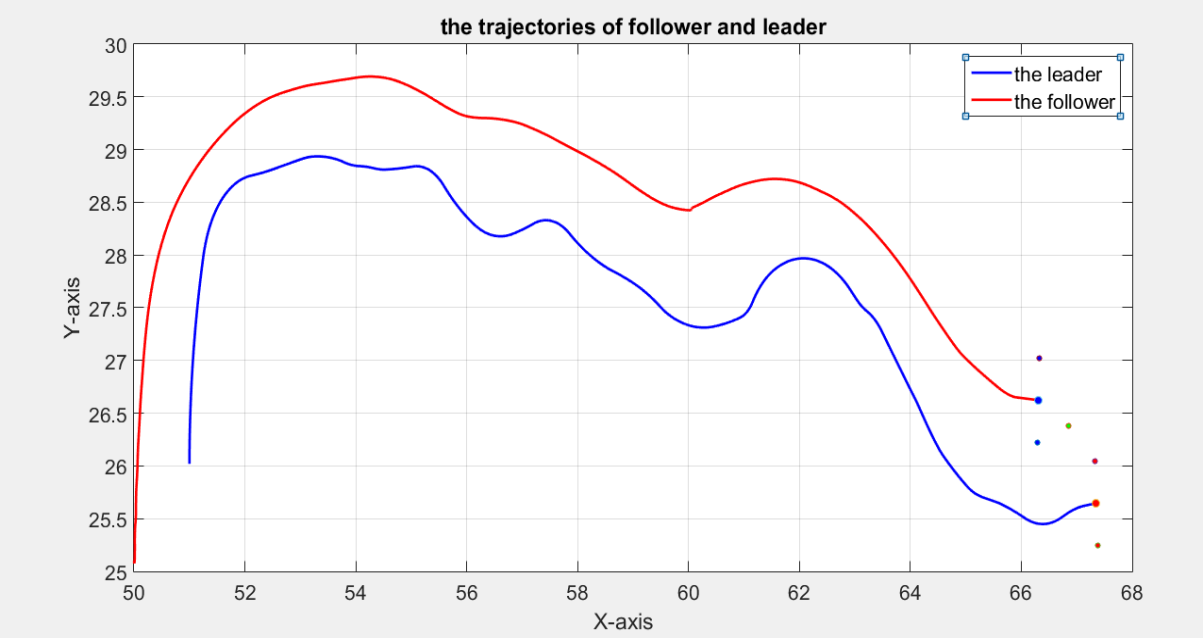

Figure 13 The trajectories of the follower and leader.

of the sphere ball are $(51,26)$ and $\pi/2$. Figure 14 shows that e_L, e_λ and m are close to zero, the camera tracks the ball and keep the ball around the center of the camera view. As a result, the follower tracks the leader at the desired position.

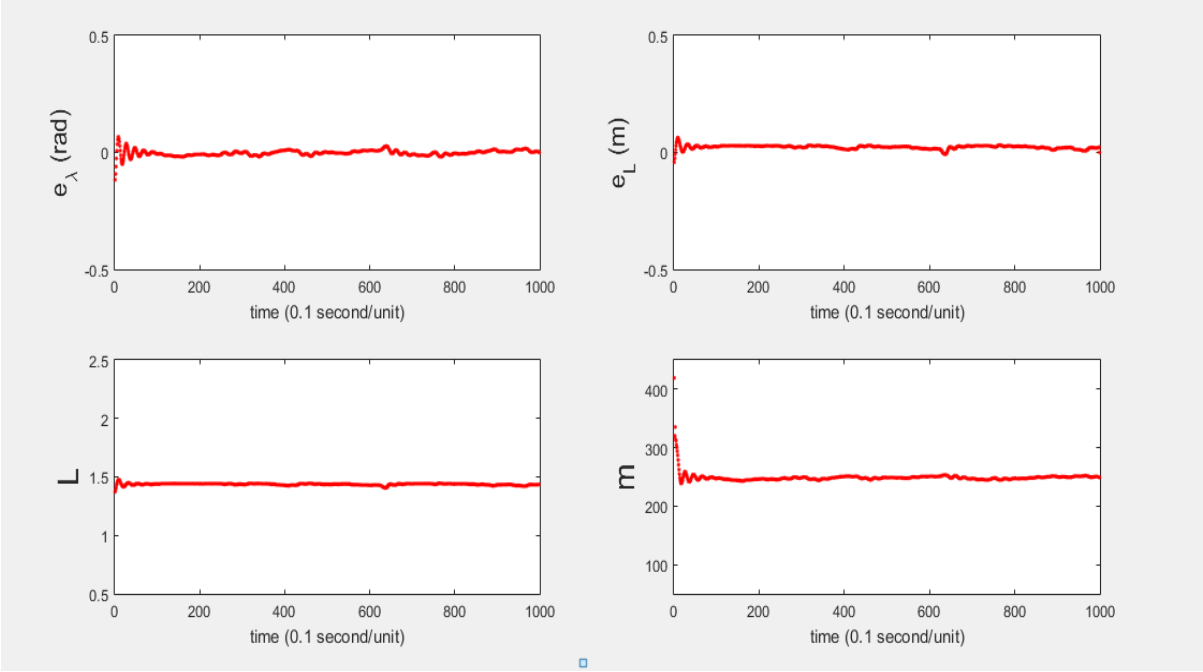

Figure 14 Simulation result. e_{λ}, e_{L}The formation error; L The relative distance between the camera and the ball; m the positon of the ball in the camera view.

4.2 Hardware and Software Designs

This section introduces the hardware and software designs which are used in the implementation.

4.2.1 Raspberry Pi 2

Raspberry Pi 2 (see Figure 15) is a cheap and powerful microcontroller with a 900MHz quad-code CPU and 1 GB RAM. Raspberry Pi 2 has excellent capability to calculate data and deal with image information. Furthermore, Raspberry Pi 2 have a friendly development environment. Users can build a project in the Linux system of Raspberry using Pi 2 Python, c, c++ and Java. Raspberry Pi 2 also supports the openCV library which is an open source library for computer vision and machine learning. In addition, there are 4 USB ports and 40 GPIO pins on Raspberry Pi 2. These interfaces make Raspberry Pi 2 connect conveniently with other devices, such as camera, sensors. In this research, Raspberry Pi 2 is used to detect the target and locate the position of the target in the camera frame.

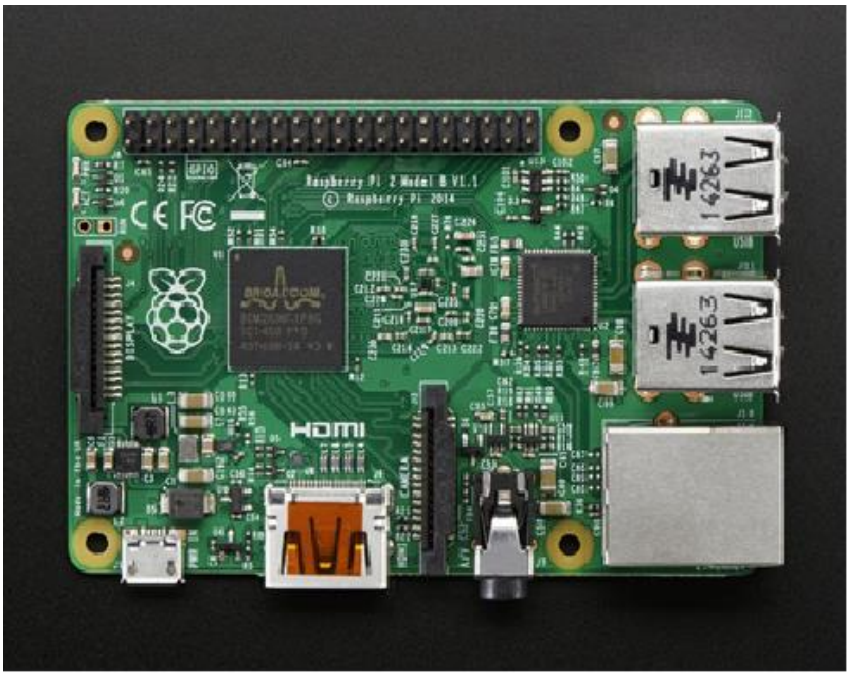

Figure 15 Raspberry Pi 2.

4.2.2 Arduino UNO

Arduino UNO is a user-friendly microcontroller built on the ship ATmega328P. As shown in Figure 16, it just has 16 I/O pins which include 6 PWM output and 16M clock speed. However, the UNO can work with lots of sensors and other devices through UART, I2C. To control motors' speed, Arduino UNO sends a value in the range (0~255) to PWM output pin. In addition, the PWM output from Arduino UNO is more stable than that from Raspberry Pi 2. In the Arduino forum, there are rich materials to help people to study and use this microcontroller. In this project, the UNO play a big role. It calculates the

Figure 16 Arduino.

wheels' speed with encoders which are installed on the motors' shafts. It calculates the target's position for the adjustment of PWM output which decides the velocities of motors. It sends the angular velocity of the camera servo to 16 channel PWM module which keeps the camera to track the target.

4.2.3 16 Channel PWM /Servo Shield

As shown in Figure 17, it is a 16-channel PWM/Servo Shield. The shield assists microcontroller to control servos by a stable PWM output. The 16 channel PWM /Servo Shield has the following advantages. It can control 16 channel and up to 992 servos using I2C. The shield is convenient to get commands from microcontrollers such as Arduino, Raspberry Pi through I2C. It can automatically control servos without keeping communication with microcontrollers so that microcontrollers can save time to execute other tasks. In this project, the shield is used to control camera's servo. The reason is Raspberry PI 2 cannot offer a stable PWM output, and Arduino needs to process data as fast as possible.

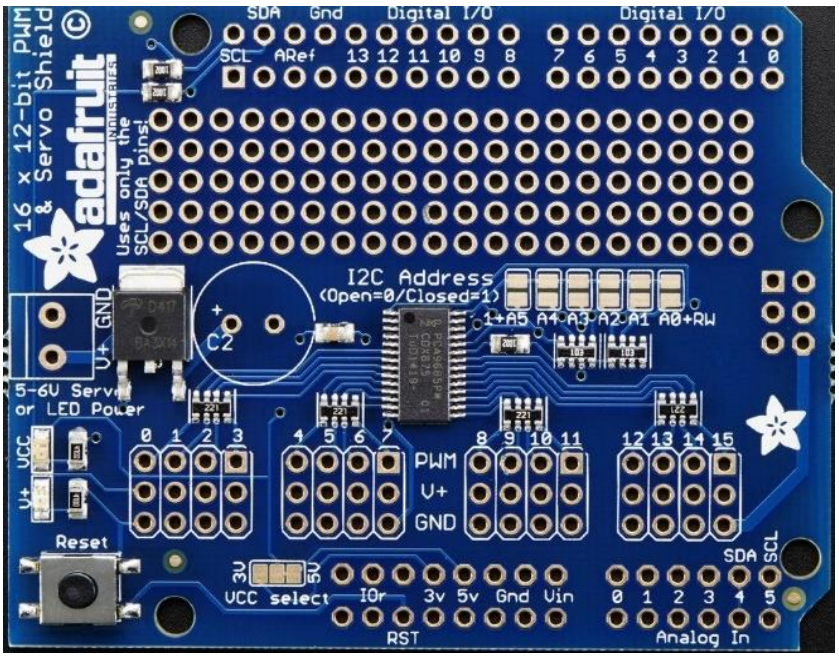

Figure 17 16-channel PWM/Servo Shield.

4.2.4 PI Camera

PI camera (see Figure 18) is an assistant device for Raspberry PI 2. The parameters of PI camera can be adjusted by Raspberry PI 2 though python command such as video formats, picture formats, and exposure modes. To compare with other webcams, PI camera is a cheaper and an excellent camera. The sensor resolution for a PI camera achieves up to 2592*1944, and its video modes can change in 1080p30, 720p60, and 640*480p60/90. PI camera is suitable to work with openCV and Raspberry PI 2. In this project, the PI camera catches the image of the target and sends the image information to Raspberry PI 2.

Figure 18 Pi camera

4.2.3 Rover 5 Motor Driver Board

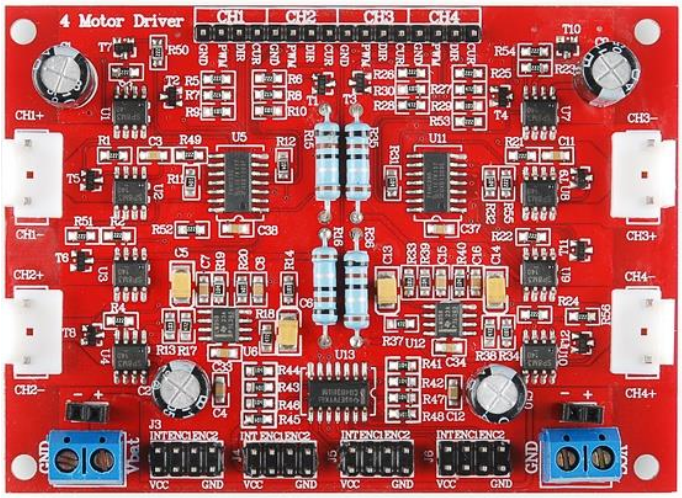

Figure 19 Rover 5 Motor Driver Board

As shown in Figure 19, it is a Rover 5 Motor Driver Board. The motor driver designed by Dagu can drive four motors with microcontrollers, such as Arduino, Raspberry Pi. The driver board can change the direction and speed of motors. In this research, the driver board connects with Arduino to control the direction and speed of wheels.

4.2.4 Lynxmotion Quadrature Motor Encoder

As shown in Figure 20, it is a Lynxmotion Quadrature Motor Encoder. It includes two output signals. The encoder has 100 cycles per revolution and 400 quadrature counts per revolution. In this research, the motor encoder accounts the speed of wheels and sends the speed data to Arduino to calculate the velocity and angular velocity of the follower robot.

Figure 20 Motor encoder

4.2.5 OpenCV

OpenCV stands for Open Source Computer Vision Library, which includes 2500 optimized algorithm on computer vision and machine learning. It supports the current main operation systems like Windows, Linux, and Mac OS. Meanwhile, it supports the following languages: C++, C, Python, Java and MATLAB. It is convenient for the user to use the algorithms of openCV on vision application so that users don't need to build a complex algorithm on the computer vision and machine learning every time. Also, the openCV is a free software. In fact, many users and companies are using openCV to develop projects and applications such as robot's navigation and face recognition. In this project, the openCV plays the main role to identify the sphere target from the camera view. The process of target detection will be described in the following section.

4.3 Detecting the Target Using Raspberry Pi 2 and OpenCV

This section focuses on the process of target detection using Raspberry Pi 2 and openCV. Raspberry Pi 2 receives image information from Pi camera and then calls for algorithms from openCV to implement these goals: color detection, smooth image, contours of images, shape recognition, locating the target's center, and area calculation in the camera frame. The remainder of this section elaborates this procedure.

4.3.1 Color Detection

Color detection refers to distinguishing an object by color. Apparently, an image consists of color components. To detect a target with a special color, it should separate an image into color components and then select the detected color components. In this research, an image is recorded by a Pi camera and sent to Raspberry Pi in an array of color components. The color element is presented by RGB color model as shown in Figure 21.a. RGB stands for red, green, and blue. In RGB color model, any color component consists of the values of these three colors. RGB color model is used to display images on electronic devices, such as a computer, phone, and tablet. However, it is difficult for people to dictate the RGB value of a color component. Therefore, it needs to convert the color space of the image into HSV color space shown in Figure 21.b. HSV stands for hue, saturation and value. The HSV color model is converted from RGB color model. To compare it with RGB color model, it is easier for people to describe a color component in HSV color model. Likewise, this conversation from RGB to HSV makes the separation of color components easily.

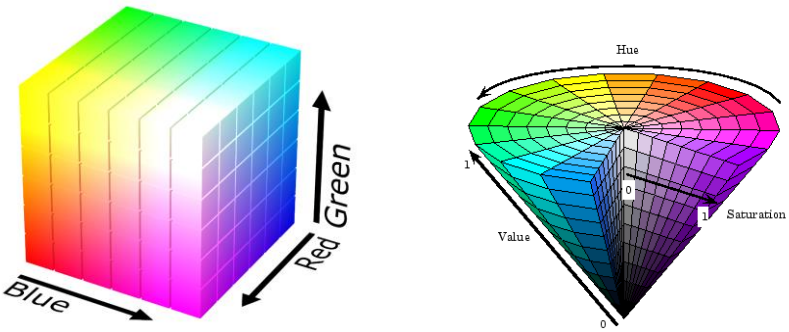

(a) RGB color space. (b) HSV color space.

Figure 21 Illustration of RGB and HSV color space.

In the implementation, the detected color is red and its HSV range is from [105, 65, 65] to [125, 255, 255]. Furthermore, the image needs to be transformed from 3-dimension to 1-dimension in order to reduce the calculation load to smoothen an image in next step. The pixel

color will be white in the detected HSV range, or the pixel color will be black. Therefore, the color image changes into a gray image. As shown in Figure 22, Our target is the red ball. The color in the detected range changes into white and other becomes black. Obviously, the color detection cannot distinguish the target from objects with the similar colors.

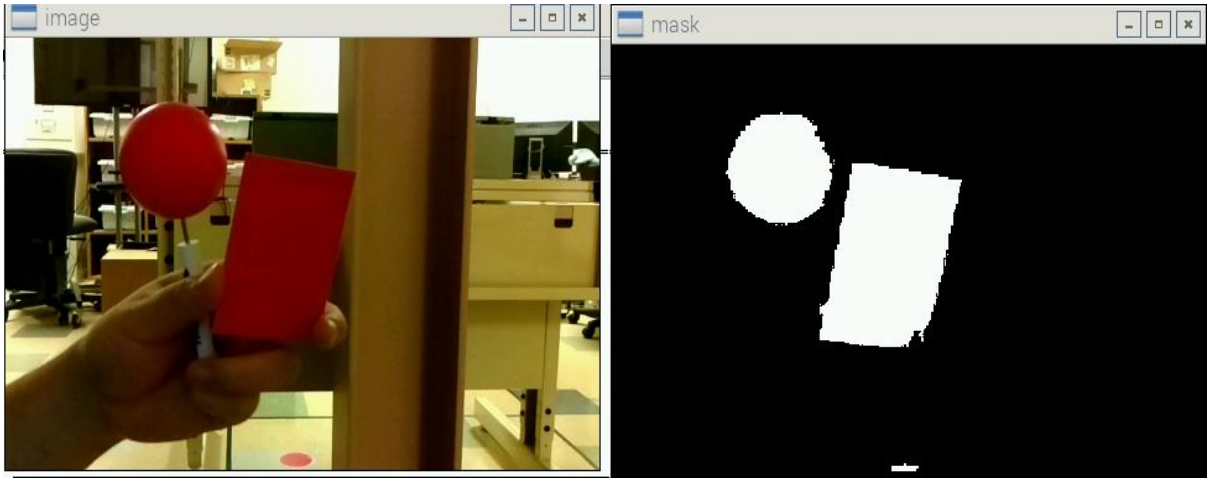

(a) (b)

Figure 22 Illustration of color detection. (a) The target ball and the noise rectangle in the normal picture. (b) The result of color detection.

4.3.2 Smooth image

As shown in Figure 22, the edges of the white blocks are irregular. Noises produce edges similar to a gear edge, and impacts correct measurement of the positions and areas of these blocks. Therefore, it is necessary to remove noises in the gray image. There are four

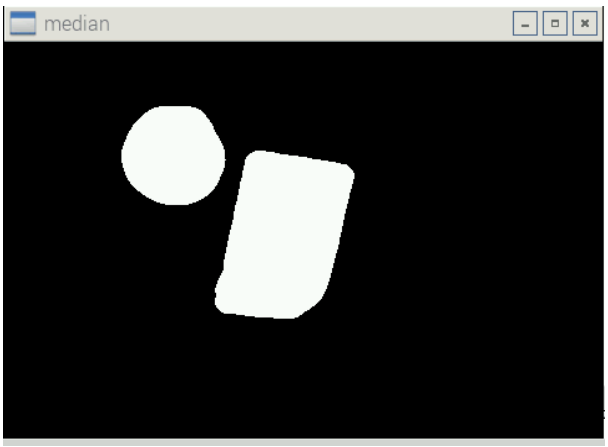

Figure 23 Illustration of Midian Filtering. The edges of blocks become smooth.

methods to reduce noise in openCV: averaging, Gaussian Filtering, Median Filtering, and Bilateral Filtering. In this research, the Median Filtering is chosen to blur an image and reduce noise. The result of the smoothened image in Median Filtering is shown in Figure 23. Clearly, from the comparison between Figure 22 and Figure 23, the edges of blocks in Figure 23 are very smooth.

4.3.3 Contours in Images

Contours mean boundaries of the detected object. The contour is an essential requirement to recognize and analyze detected shapes in openCV. The method of contours is to distinguish while block from the black background. As shown in Figure 24, the contours present the shapes of the detected target and noise.

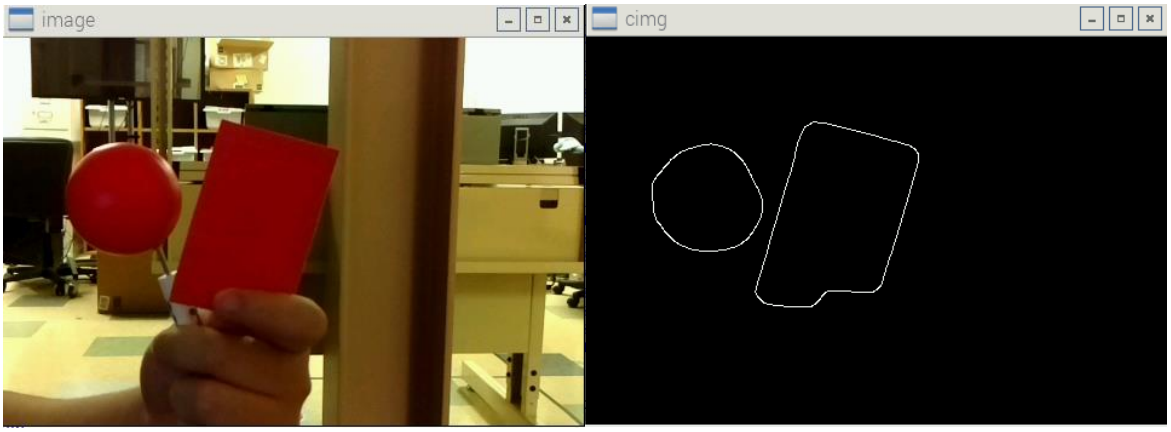

(a) (b)

Figure 24 Illustration of contours in the image. (a) Picture from camera. (b) contours of objects.

4.3.4 Shape Recognition

The shape recognition is a useful approach to distinguish the detected target from noise. Although the contours of blocks have been drawn in Figure 24, it doesn't yet distinguish the detected sphere ball from noise. As the contour of identified target is close to a circle, next step is to compare contours with a circle and then obtain the shape ratios, which means the unlike ratio between two shapes. The unlike ratio between two shapes. In this research, the contours with shape ratio less than 0.01 identify the targets to be detected. As shown in Figure 26, the shape ratio of the approximate circle is less than 0.01, and the shape ratio of noise is almost

0.1. Sometimes, noises cause objects to have similar shapes with the shape to be detected. It is difficult to select the target from noise just according to the shape ratio. The solution will be

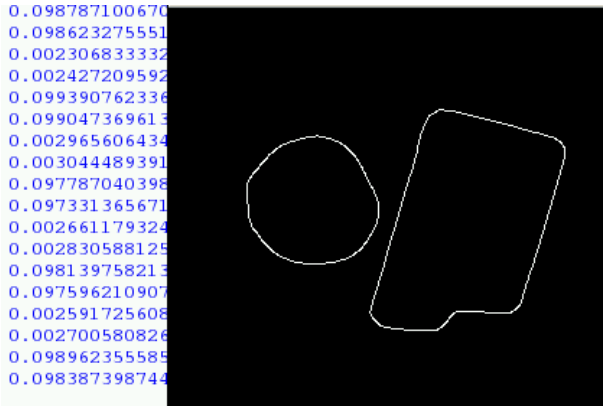

Figure 25 Illustration of shape recognition. The data (blue number) are the shape ratios of contours of blocks to a circle.

described in the following section.

4.3.5 Position and Area of the Target

Thought the algorithm of the image moments in the openCV library, the position and area of the contour are easy to be calculated. We still need to eliminate some noise which is similar with the shape of the detected target. In fact, though color detection and shape recognition, the area of noise is almost less than that of the detected target. Therefore, the detected target can be enumerated by the areas of blocks.

4.4 Implementation Result

The section focuses on the implementation result of the leader-follower tacking system using one camera and one ball. In Chapter 3, the P-controllers of the follower and camera has been built. In Section 4.3, the approach of target detection has been described. According to the diagram of hardware (see Figure 26), we build and test the hardware system. The desired

length L_d is 60 cm, and the desired angular λ_d is zero. The trajectories of the follower and the ball are shown in Figure 27.

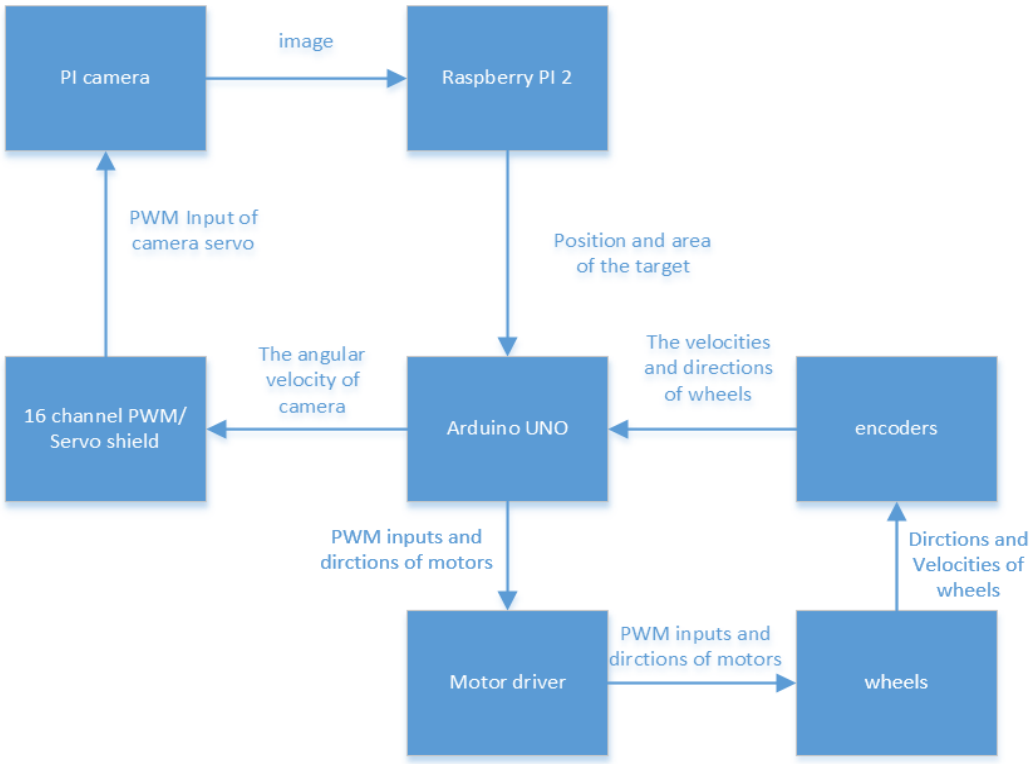

Figure 26 Illustration of the hardware connect in the implementation.

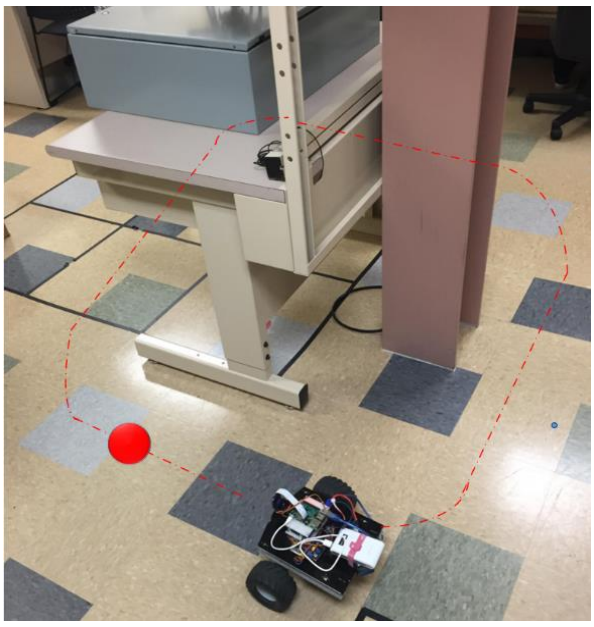

Figure 27 The trajectories of the leader and follower. The red line is the trajectory. The red ball is the detected target.

Figure 28 reports the implementation result. However, the follower tracks the ball to move and achieve the leader-follower tacking task using one camera and one ball.

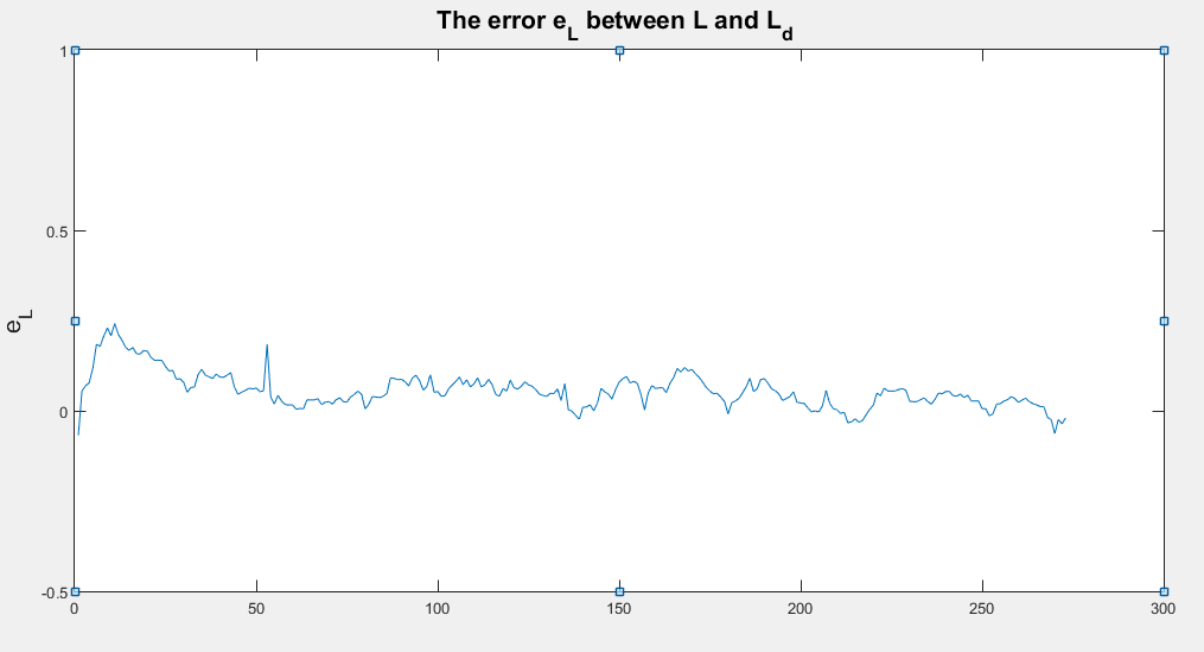

(a)

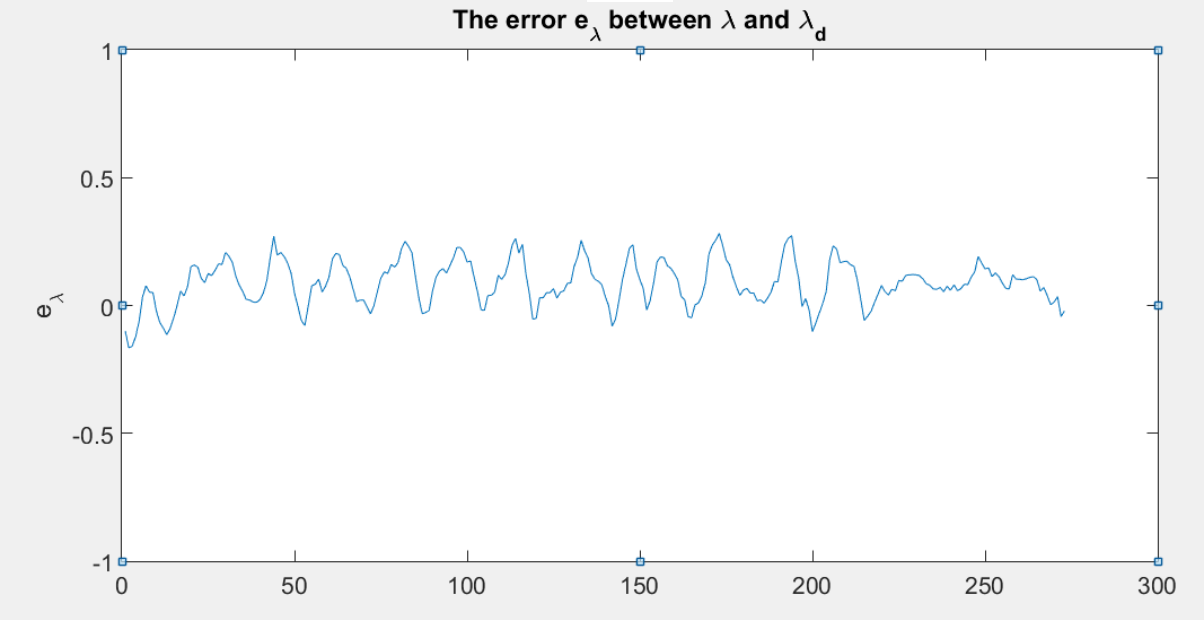

(b)

Figure 28 Implementation result. (a), (b) The formation error. The desired distance is o.6 m. the desired angle is zero.

According to the Figure 28, the follower tracks the ball to move. But we need to adjust the feedback gains to improve the performance of the leader-follower tracking system.

CHAPTER 5

CONCLUSION AND FUTURE WORK

5.1 Conclusion

In this research, we developed a method to locate a sphere using camera vision. This approach is used to estimate the relative position and bearing angular between the headings of the leader and follower. This research also builds P-controllers to realize the leader-follower tracking task using camera vision. The simulation result validates our algorithm. Then, we implemented this algorithm in a real robot system. We develop a system for the target detection by Pi camera, Raspberry Pi 2 and openCV.

The results of the simulation and implementation indicate the viability of the location method using one camera and one sphere. Meanwhile, we used our location method and built a controller for leader-follower tracking system with reasonable performance.

Our location approach just uses one camera and one ball and can provide the relative position between the camera and detected target. It is convenient for users to apply this approach on the leader-follower tracking system.

5.2 Future Work

We need still to improve the performance of the leader-follower tracking system using camera vision. The authors will design an advanced controller to replace the simply P-controller, such as the backstepping controller and adaptive controller, to achieve a better tracking performance. Finally, we achieve this task that drone tracks the robot on the ground as well as possible.

APPENDIX

DIAGRAM OF LEADER-FOLLOWER TRACKING

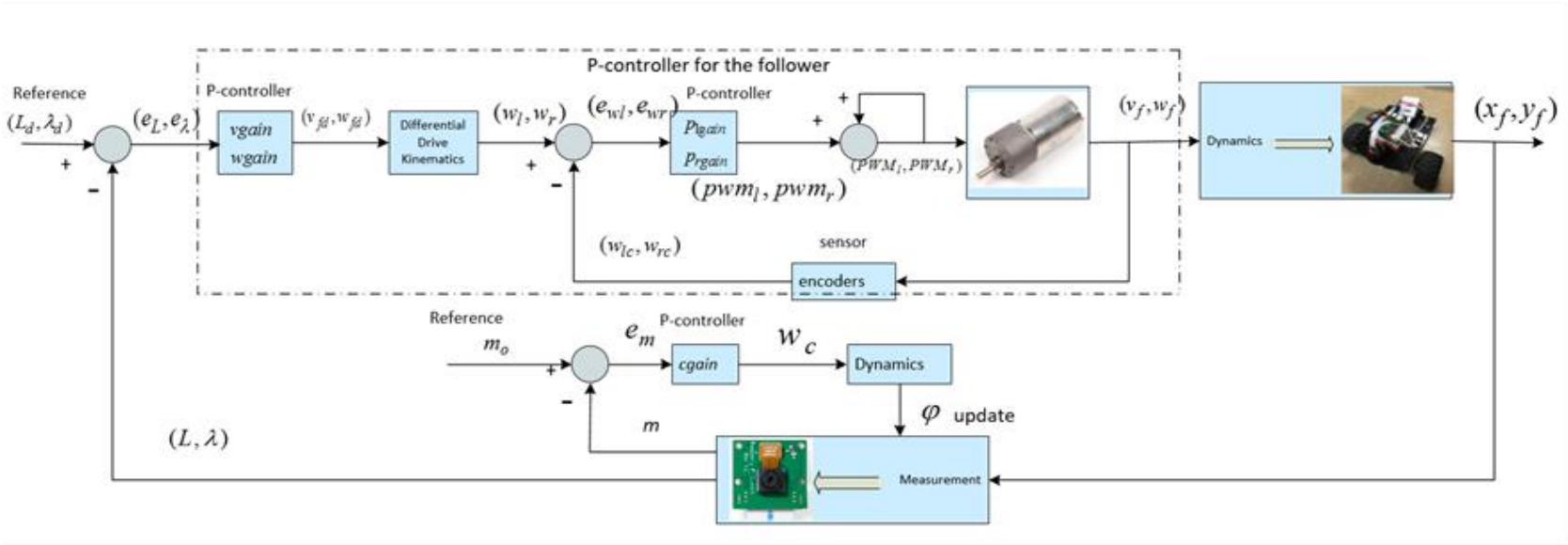

Figure 13 The diagram of the leader-follower tracking.

REFERENCES

[1] Y. Gu, M. Zhou, S. Fu and Y. Wan, "Airborne WiFi networks through directional antennae: An experimental study," *2015 IEEE Wireless Communications and Networking Conference (WCNC)*, New Orleans, LA, 2015, pp. 1314-1319.

[2] H. Kannan, V. K. Chitrakaran, D. M. Dawson and T. Burg, "Vision-Based Leader/Follower Tracking for Nonholonomic Mobile Robots," *2007 American Control Conference*, New York, NY, 2007, pp. 2159-2164.

[3] H. Poonawala, A. C. Satici, N. Gans and M. W. Spong, "Formation control of wheeled robots with vision-based position measurement," *2012 American Control Conference (ACC)*, Montreal, QC, 2012, pp. 3173-3178.

[4] G. L. Mariottini, F. Morbidi, D. Prattichizzo, G. J. Pappas and K. Daniilidis, "Leader-Follower Formations: Uncalibrated Vision-Based Localization and Control," *Proceedings 2007 IEEE International Conference on Robotics and Automation*, Roma, 2007, pp. 2403-2408.

[5] Davison, A. J., & Murray, D. W. (1998). *Mobile robot localisation using active vision* (pp. 809-825). Springer Berlin Heidelberg.

[6] Y. Fang, X. Liu and X. Zhang, "Adaptive Active Visual Servoing of Nonholonomic Mobile Robots," in *IEEE Transactions on Industrial Electronics*, vol. 59, no. 1, pp. 486-497, Jan. 2012.

[7] “Playing with your Pixy Pet!”, https://learn.adafruit.com/pixy-pet-robot-color-vision-follower-using-pixycam/playing-with-your-pet.

[8] Y. Wan, K. Namuduri, Y. Zhou and S. Fu, "A Smooth-Turn Mobility Model for Airborne Networks," in *IEEE Transactions on Vehicular Technology*, vol. 62, no. 7, pp. 3359-3370, Sept. 2013.

[9] Forsyth, D., & Ponce, J. (2003). Computer vision: A modern approach(p120-139). Upper Saddle River, NJ: Prentice Hall.

[10] Y. Wan, K. Namuduri, Y. Zhou and S. Fu, "A Smooth-Turn Mobility Model for Airborne Networks," in *IEEE Transactions on Vehicular Technology*, vol. 62, no. 7, pp. 3359-3370, Sept. 2013.

[11] Guan, J., Deboeverie, F., Slembrouck, M., van Haerenborgh, D., van Cauwelaert, D., Veelaert, P., & Philips, W. (2015). Extrinsic Calibration of Camera Networks Using a Sphere. *Sensors*, *15*(8), 18985–19005.

[12] X. Zhang, Y. Fang and X. Liu, "Motion-Estimation-Based Visual Servoing of Nonholonomic Mobile Robots," in *IEEE Transactions on Robotics*, vol. 27, no. 6, pp. 1167-1175, Dec. 2011.

[13] Dudek, Gregory, and Michael Jenkin. *Computational Principles of Mobile Robotics*(p 45-77). New York: Cambridge UP, 2000. Print.

[14] Krishnan, R. *Electric Motor Drives: Modeling, Analysis, and Control*. Upper Saddle River, NJ: Prentice Hall, 2001. Print.